

Reconstruction of cracks of different types from far field measurements

Jijun Liu and Mourad Sini*

Department of Mathematics, Southeast University, Nanjing, 210096, P.R.China. email: jjliu@seu.edu.cn
and

RICAM, Austrian Academy of Science, Altenbergerstrasse 69, Linz, A-4040, Austria. email: mourad.sini@oeaw.ac.at

SUMMARY

In this paper, we deal with the acoustic inverse scattering problem for reconstructing cracks of possibly different types from the far field map. The scattering problem models the diffraction of waves by thin two-sided cylindrical screens. The cracks are characterized by their shapes, the type of boundary conditions and the boundary coefficients (surface impedance). We give explicit formulas of the indicator function of the probe method which can be used to reconstruct the shape of the cracks, distinguish their types of boundary conditions, the two faces of each of them and reconstruct the possible material coefficients on them by using the far-field map. To test the validity of these formulas, we present some numerical implementations for a single crack, which show the efficiency of the proposed method for suitably distributed surface impedances. The difficulties for numerically recovering the properties of the crack in the concave side as well as near the tips are presented and some explanations are given. Copyright © 2009 John Wiley & Sons, Ltd.

KEY WORDS: Inverse scattering, cracks, asymptotic behavior, far-field, numerics

1. INTRODUCTION

To describe the diffraction of acoustic waves by thin two-side cylindrical screens, the scattering problems are governed by the Helmholtz equation for a crack \mathcal{C} in \mathbb{R}^2 . Let \mathcal{C} be a two dimensional open curve of class C^3 with a parametrization representation $\mathcal{C} = \{x := x(s), s \in [a, b]\}$, where $x : [a, b] \rightarrow \mathbb{R}^2$ is locally of class C^3 . We set $P = x(a)$ and $Q = x(b)$ to be the two tips of \mathcal{C} , and fix the orientation of \mathcal{C} as follows. Traveling on \mathcal{C} from P to Q , we associate to the right-hand side the sign $+$, i.e. \mathcal{C}^+ , and to the left-hand side the sign $-$, i.e. \mathcal{C}^- and we set ν to be the unit normal on \mathcal{C} oriented towards \mathcal{C}^+ . The different boundary conditions specified on \mathcal{C} represent the acoustic properties of the crack. For given incident plane waves $u^i(x) = e^{i\kappa d \cdot x}$, we consider the following

*Correspondence to: RICAM, Austrian Academy of Science, Altenbergerstrasse 69, Linz, A-4040, Austria. email: mourad.sini@oeaw.ac.at

scattering problems for total waves $u(x) = u^i(x) + u^s(x)$:

$$\text{(Dirichlet)} \begin{cases} (\Delta + \kappa^2)u = 0 & \text{in } \mathbb{R}^2 \setminus \bar{\mathcal{C}} \\ u = 0 & \text{on } \mathcal{C}^\pm \\ \lim_{r \rightarrow \infty} \sqrt{r} \left(\frac{\partial u^s}{\partial r} - i\kappa u^s \right) = 0, \end{cases} \quad (1)$$

$$\text{(Mixed)} \begin{cases} (\Delta + \kappa^2)u = 0 & \text{in } \mathbb{R}^2 \setminus \bar{\mathcal{C}} \\ u = 0 & \text{on } \mathcal{C}^+ \\ \frac{\partial u}{\partial \nu} - i\kappa \sigma_- u = 0 & \text{on } \mathcal{C}^- \\ \lim_{r \rightarrow \infty} \sqrt{r} \left(\frac{\partial u^s}{\partial r} - i\kappa u^s \right) = 0, \end{cases} \quad (2)$$

$$\text{(Robin)} \begin{cases} (\Delta + \kappa^2)u = 0 & \text{in } \mathbb{R}^2 \setminus \bar{\mathcal{C}} \\ \frac{\partial u}{\partial \nu} \pm i\kappa \sigma_\pm u = 0 & \text{on } \mathcal{C}^\pm \\ \lim_{r \rightarrow \infty} \sqrt{r} \left(\frac{\partial u^s}{\partial r} - i\kappa u^s \right) = 0, \end{cases} \quad (3)$$

where $u^s(x)$ is the scattered wave outside of \mathcal{C} , $\kappa > 0$ is the wave number and d is the direction of incident plane wave $u^i(x)$. We assume that σ^\pm are the complex-valued Hölder continuous functions of order $\beta \in (0, 1]$, $\sigma_\pm = \sigma_\pm^r + i\sigma_\pm^i$, and σ_\pm^r have positive uniform lower bounds on \mathcal{C} . These models describe the scattering problems of the cracks with different acoustic properties.

The problems (1), (2) and (3) are well-posed in some appropriate spaces, see [2, 8, 9, 10, 13, 16] for more details. More precisely, the well-posedness in Sobolev spaces can be found in [2], following the variational approach as in [16], and the well-posedness in classical Hölder spaces can be found in [8, 9, 10] where integral representations via single and angular potentials are given. Regarding the Robin problem (3) and if the surface impedances σ_\pm are equal, then a representation via a combination of single and double layer potentials is proposed in [13]. These integral representations are useful for the actual computation of the scattered fields and their corresponding far fields.

Using the asymptotic of the fundamental solution, as in [3], the scattered wave has the asymptotic behavior

$$u^s(x, d) = \frac{e^{i\kappa r}}{\sqrt{r}} u^\infty(\hat{x}, d) + O(r^{-3/2}), \quad r := |x| \rightarrow \infty, \quad (4)$$

where the function $u^\infty(\cdot, d)$ defined on the unit circle S^1 is called the far-field of the scattered wave u^s corresponding to incident direction d . We introduce a constant $\gamma_2 := \frac{e^{i\pi/4}}{\sqrt{8\pi\kappa}}$ and the fundamental solution to the Helmholtz equation in \mathbb{R}^2 :

$$\Phi(x, y) := \frac{i}{4} H_0^{(1)}(\kappa|x - y|), \quad x \neq y, x, y \in \mathbb{R}^2,$$

where $H_0^{(1)}$ is the Hankel function of the first kind of order zero. In this paper, we will consider the following

Crack reconstruction problem. Given $u^\infty(\cdot, \cdot)$ on $S^1 \times S^1$ for the scattering problems (1) or (2) or (3), reconstruct the shape of the crack \mathcal{C} , distinguish the two faces of \mathcal{C} and eventually reconstruct the surface impedances $\sigma_\pm(x)$.

REMARK 1.1

We do not know a-priori to which problem is associated the data $u^\infty(\hat{x}, d)$ on $(\hat{x}, d) \in S^1 \times S^1$. \square

The inverse problems for cracks detection have been studied by many authors. We refer to [1] for some results concerning, in particular, detection of piecewise linear cracks from one or few exterior measurements. We are interested in the detection of cracks of general shapes but using many measurements. Precisely, we are using the far field data with the aim of reconstructing the whole crack. There are several works devoted to the detection of cracks from many measurements. Among others, we shall cite [2, 5, 6] and the references therein, where the authors gave reconstruction methods to detect the shape of the cracks of Lipschitz regularity. In this paper, we shall be concerned with reconstructing complex cracks, and not only their shapes, by giving the shapes, the type of boundary conditions, distinguishing the two faces of the crack and computing the point-wise values of the complex-valued surface impedances. The price to pay is to naturally assume that the cracks have a C^3 -regularity (actually a $C^{2,\alpha}$ -regularity is enough, with any $\alpha \in (0, 1]$) and σ_\pm are Hölder continuous. With such a regularity, we provide direct formulas which link the far field data to the unknown ingredients of the cracks. These formulas reveal some geometrical information about the cracks as well as the surface impedance through an asymptotic expansion with respect to the point sources used. This asymptotic behavior shows how we should be careful to what extent these indicators can approximate the crack properties such as its shape and the possible surface impedance, from the numerical point of view. Our numerical realizations presented in the last section show that the property of the crack in the convex side can be reconstructed well, but the reconstruction in the concave side of the crack is quite limited. This phenomenon can be explained physically by the multiple reflections of the waves within the cavity, which lead to a relatively less information about the concave side in the far field pattern. In addition a suitable surface impedance distribution can improve the reconstruction in the concave part but also can destroy the one near the convex part. This fact shows how difficult it is to reconstruct numerically the shape of the crack without knowing some *a-priori* information. We wish also to point out that our formulas are valid on the points of the crack away from the tips. We believe that the indicator functions near the tips should be more singular. But such an assertion needs to be justified.

This paper is organized as follows. In section 2, we present the theoretical results related to the asymptotic formulas, with some comments on how one can use them in practical computations. In section 3 and section 4, we give the proof of these results. Finally we show extensive numerical results followed by some detailed explanations in section 5. Some preliminary results of this work have been presented in [12].

2. Statement of the results

It is well known [3] that the scattered field associated with the Herglotz incident field $v_g(x) := \int_{S^1} e^{i\kappa x \cdot d} g(d) ds(d)$, $x \in \mathbb{R}^2$ with $g \in L^2(S^1)$ is given by

$$v_g^s(x) := \int_{S^1} u^s(x, d) g(d) ds(d), \quad x \in \mathbb{R}^2 \setminus \mathcal{C},$$

and its far field is $v_g^\infty(\hat{x}) := \int_{S^1} u^\infty(\hat{x}, d) g(d) ds(d)$, $\hat{x} \in S^1$.

We will need the following identity ([3], [18])

$$u^\infty(\hat{x}, d) = -\gamma_2 \int_{\partial D} \left\{ \frac{\partial u^s(y, d)}{\partial n(y)} e^{-i\kappa \hat{x} \cdot y} - \frac{\partial e^{-i\kappa \hat{x} \cdot y}}{\partial n(y)} u^s(y, d) \right\} ds(y), \quad (5)$$

where ∂D is a closed curve containing a part of \mathcal{C} and avoiding the tips (P, Q) , and $n(y)$ is the outward normal direction of ∂D . In addition, we assume that the bounded domain surrounded by ∂D , i.e D , is such that $\mathcal{C} \subset \bar{D}$. In particular D contains the tips (P, Q) .

Before stating the main theoretical result, one remark is in order.

REMARK 2.1

Let $a \in \mathcal{C}$. The notation $a \in \mathcal{C}^\pm$ means that the sequence $\{z_p\}$, which is outside of D , tends to a from the right (+) (or, the left (-)) side of \mathcal{C} . If $a \in \mathcal{C}^+$, then D is chosen, as we did it to derive (5), so that the outward normal direction of ∂D at the point a is $\nu(a)$. If $a \in \mathcal{C}^-$, then D is chosen so that the outward normal direction of ∂D at the point a is $-\nu(a)$. \square

Assume that $\mathcal{C} \subset \subset \Omega$ for some known Ω with smooth boundary. For $a \in \Omega$, denote by $\{z_p\} \subset \Omega \setminus \bar{D}$ a sequence tending to a . For any z_p , set D_a^p to be a C^2 -regular domain such that $\bar{\mathcal{C}} \subset D_a^p$ with $z_q \in \Omega \setminus \bar{D}_a^p$ for every $q = 1, 2, \dots, p$ and that the Dirichlet interior problem on D_a^p for the Helmholtz equation is uniquely solvable. In this case, the Herglotz wave operator \mathbb{H} defined from $L^2(S^1)$ to $L^2(\partial D_a^p)$ by

$$\mathbb{H}[g](x) := v_g(x) = \int_{S^1} e^{i\kappa x \cdot d} g(d) ds(d) \quad (6)$$

is injective, compact with dense range, see [3]. Now we consider the sequence of point sources $\Phi(\cdot, z_p)$. For every p fixed, we construct two density sequences $\{g_n^p\}$ and $\{f_m^{j,p}\}$ in $L^2(S^1)$ by the Tikhonov regularization such that

$$\|v_{g_n^p} - \Phi(\cdot, z_p)\|_{L^2(\partial D_a^p)} \rightarrow 0, \quad n \rightarrow \infty, \quad (7)$$

$$\|v_{f_m^{j,p}} - \frac{\partial}{\partial x_j} \Phi(\cdot, z_p)\|_{L^2(\partial D_a^p)} \rightarrow 0, \quad m \rightarrow \infty. \quad (8)$$

We choose ∂D , as we did it to derive (5), to contain a part of \mathcal{C} surrounding the fixed point a , such that $\{z_p\} \subset \Omega \setminus \bar{D}$ (for p large enough) and $\mathcal{C} \subset \bar{D} \subset D_a^p$. Since both $v_{g_n^p}$ and $\Phi(\cdot, z_p)$ satisfy the same Helmholtz equation in D_a^p , (7) implies that

$$\|v_{g_n^p} - \Phi(\cdot, z_p)\|_{H^{\frac{1}{2}}(\partial D)} \rightarrow 0, \quad n \rightarrow \infty \quad (9)$$

$$\left\| \frac{\partial}{\partial n} v_{g_n^p} - \frac{\partial}{\partial n} \Phi(\cdot, z_p) \right\|_{H^{-\frac{1}{2}}(\partial D)} \rightarrow 0, \quad m \rightarrow \infty \quad (10)$$

Similarly, it follows from (8) that

$$\|v_{f_m^{j,p}} - \frac{\partial}{\partial x_j} \Phi(\cdot, z_p)\|_{H^{\frac{1}{2}}(\partial D)} \rightarrow 0, \quad m \rightarrow \infty \quad (11)$$

$$\left\| \frac{\partial}{\partial n} v_{f_m^{j,p}} - \frac{\partial}{\partial n} \left(\frac{\partial}{\partial x_j} \Phi(\cdot, z_p) \right) \right\|_{H^{-\frac{1}{2}}(\partial D)} \rightarrow 0, \quad m \rightarrow \infty \quad (12)$$

Multiplying (5) by $f_m^{j,p}(d)g_n^p(\hat{x})$ and integrating over $S^1 \times S^1$, we have

$$\begin{aligned}
& - \int_{S^1} \int_{S^1} u^\infty(-\hat{x}, d) f_m^{j,p}(d) g_n^p(\hat{x}) ds(\hat{x}) ds(d) \\
= & \gamma_2 \int_{\partial D} \left\{ \int_{S^1} \frac{\partial u^s(y, d)}{\partial n(y)} f_m^{j,p}(d) ds(d) \cdot \int_{S^1} e^{i\kappa \hat{x} \cdot y} g_n^p(\hat{x}) ds(\hat{x}) - \right. \\
& \left. \int_{S^1} \frac{\partial e^{i\kappa \hat{x} \cdot y}}{\partial n(y)} g_n^p(\hat{x}) ds(\hat{x}) \cdot \int_{S^1} u^s(y, d) f_m^{j,p}(d) ds(d) \right\} ds(y) \\
= & \gamma_2 \int_{\partial D} \left\{ \frac{\partial v_{f_m^{j,p}}^s}{\partial n(y)}(y) v_{g_n^p}^i(y) - \frac{\partial v_{g_n^p}^i}{\partial n(y)}(y) v_{f_m^{j,p}}^s(y) \right\} ds(y). \tag{13}
\end{aligned}$$

From (11), (12) and (13), we have from the Green formula that

$$\begin{aligned}
& \lim_{n \rightarrow \infty} \int_{S^1} \int_{S^1} u^\infty(-\hat{x}, d) f_m^{j,p}(d) g_n^p(\hat{x}) ds(\hat{x}) ds(d) \\
= & \gamma_2 \int_{\partial D} \left\{ v_{f_m^{j,p}}^s \frac{\partial \Phi(y, z_p)}{\partial n(y)} - \frac{\partial v_{f_m^{j,p}}^s}{\partial n(y)} \Phi(y, z_p) \right\} ds(y) = \gamma_2 v_{f_m^{j,p}}^s(z_p), \tag{14}
\end{aligned}$$

where $v_{f_m^{j,p}}^s(\cdot)$ is the scattered wave corresponding to incident wave $v_{f_m^{j,p}}^i(x) = \mathbb{H}[f_m^{j,p}](x)$.

Denote by $E_j^s(x, z_p)$ the scattered wave corresponding to the incident wave $\frac{\partial \Phi(x, z_p)}{\partial x_j}$, which is well defined for every $x \in \mathbb{R}^2 \setminus \bar{\mathcal{C}}$. Then it follows from (10), (11), the well posedness of the direct scattering problem and the interior estimate of boundary value problem that

$$E_j^s(x, z_p) = \lim_{m \rightarrow \infty} v_{f_m^{j,p}}^s(x), \quad x \in \mathbb{R}^2 \setminus \bar{D}. \tag{15}$$

Finally, it follows from (14) that

$$\lim_{m \rightarrow \infty} \lim_{n \rightarrow \infty} \int_{S^1} \int_{S^1} u^\infty(-\hat{x}, d) f_m^{j,p}(d) g_n^p(\hat{x}) ds(\hat{x}) ds(d) = \gamma_2 E_j^s(z_p, z_p). \tag{16}$$

We set

$$I_j(z_p) := \frac{1}{\gamma_2} \lim_{m \rightarrow \infty} \lim_{n \rightarrow \infty} \int_{S^1} \int_{S^1} u^\infty(-\hat{x}, d) f_m^{j,p}(d) g_n^p(\hat{x}) ds(\hat{x}) ds(d). \tag{17}$$

Let us mention that the construction of $f_m^{j,p}$ and g_m^p is independent of the unknown crack. Hence $I_j(z_p)$ is computable from our data only.

The reconstruction of the crack \mathcal{C} as well as its eventual surface impedance is established by analyzing the behavior of (16) by taking $z_p \rightarrow a$ for the test point a . For this process, we need the C^3 smooth assumption on \mathcal{C} . Precisely, for every point $a \in \mathcal{C} \setminus \{P, Q\}$, there exists a rigid transformation of coordinates under which the image of a is $\mathbf{0}$ and a function $f_a \in C^3(-r, r)$ such that

$$f_a(0) = \frac{df_a}{dx}(0) = 0, \quad D \cap B(\mathbf{0}, r) = \{(x_1, x_2) \in B(\mathbf{0}, r); x_2 < f_a(x_1)\} \tag{18}$$

in terms of the new coordinates where $B(\mathbf{0}, r)$ is the disc of center $\mathbf{0}$ with radius r . For the point $a \in \mathcal{C}$, we choose the sequence $\{z_p\}_{p \in \mathbb{N}}$ included in $C_{a, \theta}$, where $C_{a, \theta}$ is a cone with center a , angle $\theta \in [0, \frac{\pi}{2})$ and axis $\nu(a)$. The answer to the inverse problem of crack detection is based on the following theorem related to the asymptotic of the indicator functions $I_j(z_p)$.

THEOREM 2.2

Assume that \mathcal{C} is of class C^3 and $\sigma_{\pm} := \sigma_{\pm}^r + i\sigma_{\pm}^i$ are Hölder continuous functions with positive lower bounds for σ_{\pm}^r . Then we have the following asymptotic formulas:

1. $\Re(I_j(z_p)) =$

$$\begin{cases} \frac{\pm\nu_j(a)}{4\pi|(z_p-a)\cdot\nu(a)} \pm \frac{\nu_j(a)}{\pi}\kappa\sigma_{\pm}^i(a)\ln(|(z_p-a)\cdot\nu(a)|) + O(1), & a \in \mathcal{C}^{\pm} \setminus \{P, Q\} \\ \text{(for the impedance boundary conditions),} \\ \frac{\mp\nu_j(a)}{4\pi|(z_p-a)\cdot\nu(a)} + O(1), & a \in \mathcal{C}^{\pm} \setminus \{P, Q\} \\ \text{(for the Dirichlet boundary conditions).} \end{cases} \quad (19)$$

2.

$$\Im(I_j(z_p)) = \begin{cases} \frac{\mp\nu_j(a)}{\pi}\kappa\sigma_{\pm}^r\ln(|(z_p-a)\cdot\nu(a)|) + O(1), & a \in \mathcal{C}^{\pm} \setminus \{P, Q\} \\ \text{(for the impedance boundary conditions),} \\ O(1), & a \in \mathcal{C}^{\pm} \setminus \{P, Q\} \\ \text{(for the Dirichlet boundary conditions).} \end{cases} \quad (20)$$

□

REMARK 2.3

The needed regularity condition for \mathcal{C} is actually $C^{2,\alpha}$, with any $\alpha \in (0, 1]$. □

Next, let us give some comments explaining how to use the above asymptotic formulas to extract the information about the crack. The formulas (19) and (20) can be used in the following ways.

- Determine a sample of points on the crack and find the normal direction on these points. The points can be given by numerically solving $|\Re I_j(z)| = C$ for constant C large enough. The normals are obtained as follows:

$$\nu(a) = \pm(t\sqrt{\frac{1}{1+t^2}}, \sqrt{\frac{1}{1+t^2}}), \quad \text{where } t := \lim_{z_p \rightarrow a} \frac{\Re I_1(z_p)}{\Re I_2(z_p)}.$$

- Distinguish the parts where we have Dirichlet or Impedance type of boundary conditions. This is a consequence of the following identities for $a \in \mathcal{C}^{\pm} \setminus \{P, Q\}$ and any given $s \in (0, 1)$:

$$\lim_{z_p \rightarrow a} \frac{|\Im I_j(z_p)|}{|\ln(|(z_p-a)\cdot\nu(a)|)|^s} = \begin{cases} \infty, & \text{Impedance boundary,} \\ 0, & \text{Dirichlet boundary.} \end{cases} \quad (21)$$

- In case of impedance type boundary conditions, we can reconstruct the real and the imaginary parts surface impedance σ_{\pm} using the following formulas:

$$\sigma_{\pm}^r(a) = \lim_{z_p \rightarrow a} \frac{\pi \sum_{j=1}^2 \mp \nu_j(a) \Im I_j(z_p)}{\kappa \ln(|(z_p-a)\cdot\nu(a)|)} \quad (22)$$

and

$$\sigma_{\pm}^i(a) = \lim_{z_p \rightarrow a} \frac{\pi \sum_{j=1}^2 \pm \nu_j(a) \Re I_j(z_p) - \frac{1}{4|(z_p-a)\cdot\nu(a)|}}{\kappa \ln(|(z_p-a)\cdot\nu(a)|)}. \quad (23)$$

- The formula (22), rewritten as

$$\pm \sigma_{\pm}^r(a) = - \lim_{z_p \rightarrow a} \frac{\pi \sum_{j=1}^2 \nu_j(a) \Im I_j(z_p)}{\kappa \ln(|(z_p - a) \cdot \nu(a)|)}, \quad (24)$$

enables us to know if $a \in \mathcal{C}^+$ or $a \in \mathcal{C}^-$, i.e to distinguish between the two faces of the crack. Indeed, since $\sigma_{\pm}^r(a) > 0$, then if the right-hand side of (24) is positive then $a \in \mathcal{C}^+$ and if it is negative then $a \in \mathcal{C}^-$. We can also use the first equation of (19) as follows:

$$\lim_{z_p \rightarrow a} \sum_{j=1}^2 \nu_j(a) \Re I_j(z_p) = \begin{cases} +\infty, & \text{on } \mathcal{C}_+ \\ -\infty, & \text{on } \mathcal{C}_- \end{cases} \quad (25)$$

for the impedance boundary condition and

$$\lim_{z_p \rightarrow a} \sum_{j=1}^2 \nu_j(a) \Re I_j(z_p) = \begin{cases} -\infty, & \text{on } \mathcal{C}_+ \\ +\infty, & \text{on } \mathcal{C}_- \end{cases} \quad (26)$$

for the Dirichlet boundary condition.

3. Proof of Theorem 2.2

In this section, we give the proof of Theorem 2.2 for the impedance case since for the Dirichlet case the proof is similar. We consider only the case $j = 2$ of Theorem 2.2. The case $j = 1$ can be handled in a similar way with some appropriate changes.

We recall that for any given point $a \in \mathcal{C}$, we distinguish two possibilities, $a \in \mathcal{C}^+$ or $a \in \mathcal{C}^-$. If $a \in \mathcal{C}^+$, then D is chosen, as we did it to derive (5), so that the outward normal direction of ∂D at the point a is $\nu(a)$. Hence recalling (18), we firstly take the rotation R_a^+ and the translation M_a such that $R_a^+(\nu(a)) = (0, 1)$, $R_a^+(a) + M_a = \mathbf{0}$ in the new coordinate system \tilde{x} . Under the transformation $\tilde{x} := \mathbb{T}^+(x) := R_a^+(x) + M_a(x)$, it follows that $\mathbb{T}^+(\nu(a)) = (0, 1)$, $\mathbb{T}^+(a) = \mathbf{0}$. If $a \in \mathcal{C}^-$, then D is chosen so that the outward normal direction of ∂D is $-\nu(a)$. In this case, we take the rotation R_a^- and the same translation M_a such that $R_a^-(-\nu(a)) = (0, 1)$. However, it is easy to see that $R_a^- = -R_a^+$. We set $\mathbb{T}^-(x) = R_a^-(x) + M_a(x)$. Hence in both cases, either $a \in \mathcal{C}^+$ or $a \in \mathcal{C}^-$, after the corresponding transform of coordinates, a is mapped to the origin and the normal is mapped to the vector $(0, 1)$ which is oriented towards the exterior of D , $(\bar{D} \supset \mathcal{C})$.

Introduce the following two problems under the transformed coordinate $\tilde{x} = (\tilde{x}_1, \tilde{x}_2)$ for any given $\tilde{z} = (\tilde{z}_1, \tilde{z}_2) \in \mathbb{R}_+^2$:

$$\begin{cases} \Delta \tilde{w}_{\sigma(a)}^{\pm} = 0, & \tilde{x} \in \mathbb{R}_+^2 \\ \left(\frac{\partial}{\partial \tilde{x}_2} \tilde{w}_{\sigma(a)}^{\pm} + i\kappa\sigma(a) \tilde{w}_{\sigma(a)}^{\pm} \right) (\tilde{x}, \tilde{z})|_{\tilde{x}_2=0} = - \left(\frac{\partial}{\partial \tilde{x}_2} + i\kappa\sigma(a) \right) \nabla \Gamma(\tilde{x}, \tilde{z}) \cdot \tau^{\pm}|_{\tilde{x}_2=0}, \end{cases} \quad (27)$$

$$\begin{cases} \Delta \tilde{w}_D^{\pm} = 0, & \tilde{x} \in \mathbb{R}_+^2, \\ \tilde{w}_D^{\pm}(\tilde{x}, \tilde{z})|_{\tilde{x}_2=0} = -\nabla \Gamma(\tilde{x}, \tilde{z}) \cdot \tau^{\pm}|_{\tilde{x}_2=0}, \end{cases} \quad (28)$$

respectively, where $\Gamma(\tilde{x}, \tilde{z}) = \frac{1}{2\pi} \ln \frac{1}{|\tilde{x} - \tilde{z}|}$ and the subscript D in $\tilde{w}_D^{\pm}(\tilde{x}, \tilde{z})$ refers to the Dirichlet boundary condition in (28). The vector τ^{\pm} is given by $\tau^{\pm} := R_a^{\pm}(0, 1) = \pm(-\nu_1(a), \nu_2(a))$. Moreover, define four functions $w_{\sigma(a)}^{\pm}(x, z)$ and $w_D^{\pm}(x, z)$ by

$$w_{\sigma(a)}^{\pm}(x, z) := \tilde{w}_{\sigma(a)}^{\pm}(\tilde{x}, \tilde{z}), \quad w_D^{\pm}(x, z) := \tilde{w}_D^{\pm}(\tilde{x}, \tilde{z}).$$

Now, we state two propositions which will be used in the proof of Theorem 2.1, while their proofs will be given in section 4.

PROPOSITION 3.1

The asymptotic behavior of $E_2^s(z, z)$ can be stated in the two cases as follows.

Case 1. Impedance boundary condition. Let $a \in \mathcal{C}^\pm \setminus \{P, Q\}$, then there exist $\delta(a) > 0$ and $C > 0$ such that

$$\left| E_2^s(z, z) - w_{\sigma(a)}^\pm(z, z) \right| \leq C \quad (29)$$

for $z \in B_+(a, \delta(a)) \cap C_{a, \theta}$, where $B_+(a, \delta(a)) := B(a, \delta(a)) \cap (\mathbb{R}^2 \setminus D)$ and $B(a, \delta(a))$ is the ball of center a and radius $\delta(a)$.

Case 2. Dirichlet boundary condition. If $a \in \mathcal{C}^+ \setminus \{P, Q\}$, then the asymptotic behavior is obtained by replacing $w_{\sigma(a)}^\pm$ in (29) by w_D^\pm . \square

PROPOSITION 3.2

The functions $w_{\sigma(a)}^\pm(\tilde{x}, \tilde{z})$ have the following explicit forms

$$\begin{aligned} \tilde{w}_{\sigma(a)}^\pm(\tilde{x}, \tilde{z}) &= \frac{\pm \nu_2(a)}{4\pi} \int_{\mathbb{R}} e^{i(\tilde{x}_1 - \tilde{z}_1)\xi_1} e^{-(\tilde{x}_2 + \tilde{z}_2)|\xi_1|} \frac{|\xi_1| + i\kappa\sigma(a)}{|\xi_1| - i\kappa\sigma(a)} d\xi_1 \mp \\ & i \frac{\nu_1(a)}{4\pi} \int_{\mathbb{R}} e^{i(\tilde{x}_1 - \tilde{z}_1)\xi_1} e^{-(\tilde{x}_2 + \tilde{z}_2)|\xi_1|} \frac{\xi_1}{|\xi_1|} \frac{|\xi_1| + i\kappa\sigma(a)}{|\xi_1| - i\kappa\sigma(a)} d\xi_1, \end{aligned} \quad (30)$$

while the functions $\tilde{w}_D^\pm(\tilde{x}, \tilde{z})$ have the forms

$$\tilde{w}_D^\pm(\tilde{x}, \tilde{z}) = \mp \frac{\nu_2(a)}{4\pi} \int_{\mathbb{R}} e^{i(\tilde{x}_1 - \tilde{z}_1)\xi_1} e^{-(\tilde{x}_2 + \tilde{z}_2)|\xi_1|} d\xi_1 \pm i \frac{\nu_1(a)}{4\pi} \int_{\mathbb{R}} e^{i(\tilde{x}_1 - \tilde{z}_1)\xi_1} e^{-(\tilde{x}_2 + \tilde{z}_2)|\xi_1|} \frac{\xi_1}{|\xi_1|} d\xi_1. \quad (31)$$

In addition, taking $\tilde{x}_1 = \tilde{z}_1$, we have for \tilde{x}_2 and \tilde{z}_2 near 0 that

$$\tilde{w}_{\sigma(a)}^\pm(\tilde{x}, \tilde{z}) = \pm \frac{\nu_2(a)}{2\pi(\tilde{x}_2 + \tilde{z}_2)} \mp \frac{i\kappa\nu_2(a)\sigma(a)}{\pi} \ln(\tilde{x}_2 + \tilde{z}_2) + O(1), \quad (32)$$

$$\tilde{w}_D^\pm(\tilde{x}, \tilde{z}) = \mp \frac{\nu_2(a)}{2\pi(\tilde{x}_2 + \tilde{z}_2)} + O(1). \quad (33)$$

\square

Coming back to the original coordinates (x, z) , we have from (32) and (33) that

$$w_{\sigma(a)}^\pm(z, z) = \pm \frac{\nu_2(a)}{4\pi|(z-a) \cdot \nu(a)|} \mp \frac{i\kappa\sigma(a)\nu_2(a)}{\pi} \ln(|(z-a) \cdot \nu(a)|) + O(1)$$

and

$$w_D^\pm(z, z) = \mp \frac{\nu_2(a)}{4\pi(z-a) \cdot \nu(a)} + O(1)$$

for z near a . Finally, the proof of Theorem 2.2 is done by directly combining Proposition 3.1 and the above two asymptotic expansions. \square

4. Proof of the two propositions.

This section is dedicated to the proofs of Proposition 3.1 and Proposition 3.2 used in section 3.

4.1. Proof of Proposition 3.1.

We consider the case where $a \in \mathcal{C}^+ \setminus \{P, Q\}$, i.e., z_p tends to a from the positive side of \mathcal{C} . The case $a \in \mathcal{C}^-$ can be done by replacing $\nu(a)$ by $-\nu(a)$. Indeed, if $a \in \mathcal{C}^-$ then due to the choice of D we have $n = -\nu$ near a . However, on \mathcal{C}^- we have the boundary condition $(\frac{\partial}{\partial \nu} - i\kappa)(E_2^s(x, z_p) + \frac{\partial \Phi(x, z_p)}{\partial x_2}) = 0$ for the total fields $E_2^s(x, z_p) + \frac{\partial \Phi(x, z_p)}{\partial x_2}$. Hence we can write $(\frac{\partial}{\partial n} + i\kappa)(E_2^s(x, z_p) + \frac{\partial \Phi(x, z_p)}{\partial x_2}) = 0$ near a . This means that for both $a \in \mathcal{C}^+$ and $a \in \mathcal{C}^-$, we have the same (sign for the) boundary condition near a . The difference in the sign, in Proposition 3.1, comes from the different rotations, R_a^+ for $a \in \mathcal{C}^+$ and R_a^- for $a \in \mathcal{C}^-$, we need to use to obtain the asymptotic and the fact that $R_a^+ = -R_a^-$. The precise point of the proof where we need to make the change is indicated in Remark 4.5, see Section 4.3.

In the sequel, we use the notation ν for the normal of ∂D (instead of n) since $n = \nu$ near the point a , $a \in \mathcal{C}^+$.

Let $\tilde{E}^s(x, z_p)$ be the solution of

$$\begin{cases} (\Delta + \kappa^2)\tilde{E}^s(x, z_p) = 0 & \text{in } \mathbb{R}^2 \setminus \bar{D} \\ (\frac{\partial}{\partial \nu} + i\kappa\sigma(x))\tilde{E}^s(x, z_p) = -(\partial_\nu + i\kappa\sigma(x))\frac{\partial}{\partial x_2}\Phi(x, z_p) & \text{on } \partial D \\ \tilde{E}^s(\cdot, z) \text{ satisfies the Sommerfeld radiation condition.} \end{cases} \quad (34)$$

Note that σ has been defined just on \mathcal{C} . We extend it to ∂D as a Hölder continuous function and denote it again by σ .

Part one. $\tilde{E}^s(x, z)$ is the dominant part of $E^s(x, z)$ for x, z near a .

Define $\tilde{H}_\sigma(x, z) := \tilde{E}^s(x, z) + \frac{\partial}{\partial x_2}\Phi(x, z)$. Then it satisfies

$$\begin{cases} (\Delta + \kappa^2)\tilde{H}_\sigma(x, z) = -\nabla\delta(x, z) \cdot (0, 1), & \text{in } \mathbb{R}^2 \setminus \bar{D} \\ (\frac{\partial}{\partial \nu} + i\kappa\sigma)\tilde{H}_\sigma(x, z) = 0, & \text{on } \partial D \\ \tilde{H}_\sigma(\cdot, z) \text{ satisfies the Sommerfeld radiation condition.} \end{cases} \quad (35)$$

Similarly, we set $H_\sigma(x, z) := E^s(x, z) + \frac{\partial}{\partial x_2}\Phi(x, z)$. Hence $W := H_\sigma - \tilde{H}_\sigma$ satisfies

$$\begin{cases} (\Delta + \kappa^2)W(x, z) = 0 & \text{in } \mathbb{R}^2 \setminus \bar{D} \\ (\frac{\partial}{\partial \nu} + i\kappa\sigma)W(x, z) = 0, & \text{on } \mathcal{C} \cap \partial D. \end{cases} \quad (36)$$

Let B be a disc with center a and radius $r > 0$. The arguments in [4] show that $H_{\sigma(a)}$ and $\tilde{H}_{\sigma(a)}$ satisfy for $x, z \in B \setminus D$ the estimates

$$|H_{\sigma(a)}(x, z)|, |\tilde{H}_{\sigma(a)}(x, z)| \leq \frac{C}{|x - z|} \quad \text{and} \quad |\nabla_x H_{\sigma(a)}(x, z)|, |\nabla_x \tilde{H}_{\sigma(a)}(x, z)| \leq \frac{C}{|x - z|^2}, \quad (37)$$

where C is a positive constant. With these properties and (36), we see that $W(\cdot, z)$ satisfies the Helmholtz equation in $B \setminus \bar{D}$, the impedance boundary condition $(\frac{\partial}{\partial \nu} + i\kappa\sigma)W(\cdot, z) = 0$ on $\mathcal{C} \cap \partial D$ and $(\frac{\partial}{\partial \nu} + i\kappa\sigma)W(\cdot, z)$ has a bounded $H^{-1/2}(\partial(B \setminus \bar{D}) \setminus (\mathcal{C} \cap \partial D))$ -norm on $\partial(B \setminus \bar{D}) \setminus (\mathcal{C} \cap \partial D)$ for z near a . We choose B small enough so that κ^2 is not an eigenvalue for the impedance problem satisfied by $W(\cdot, z)$ on $B \setminus \bar{D}$. Note that if the surface impedance is not real then there is no eigenvalue associated to the impedance boundary value problem. From the well posed-ness of this

problem in Sobolev spaces, see [16], we deduce in particular that $\|W(\cdot, z)\|_{H^1(B \setminus \bar{D})}$ is bounded with respect to z near a .

We set G to be the Green's function for $\Delta + \kappa^2$ in $B \setminus \bar{D}$ with a homogeneous Neumann condition on $\partial(B \setminus D)$. An integration by parts shows that

$$W(x, z_p) = - \int_{\partial(B \setminus \bar{D})} G(y, x) \frac{\partial}{\partial \nu} W(y, z_p) ds(y), \text{ for } x, z_p \in B \setminus \bar{D}. \quad (38)$$

Using the boundary condition in (36), we obtain

$$W(x, z_p) = - \int_{\partial(B \setminus \bar{D}) \setminus (\mathcal{C} \setminus \partial D)} G(y, x) \frac{\partial}{\partial \nu} W(y, z_p) ds(y) + i\kappa \int_{\mathcal{C} \setminus \partial D} \sigma(y) G(y, x) W(y, z_p) ds(y), \quad (39)$$

for $x \in \partial(B \setminus \bar{D})$, $z_p \in B \setminus \bar{D}$.

From the point-wise estimate in (37) and the corresponding ones of G , we deduce that

$$\int_{\partial(B \setminus \bar{D}) \setminus (\mathcal{C} \setminus \partial D)} G(y, x) \frac{\partial}{\partial \nu} W(y, z_p) ds(y)$$

is bounded for x, z_p near a , since a is away from $\partial(B \setminus \bar{D}) \setminus (\mathcal{C} \setminus \partial D)$. The Cauchy-Schwartz inequality and the boundedness of σ give

$$\left| \int_{\mathcal{C} \setminus \partial D} \sigma(y) G(y, x) W(y, z_p) ds(y) \right| \leq \max_{y \in \mathcal{C}} |\sigma(y)| \|G(\cdot, x)\|_{L^2(\mathcal{C} \setminus \partial D)} \|W(\cdot, z_p)\|_{L^2(\mathcal{C} \setminus \partial D)}.$$

As we have shown above, $\|W(\cdot, z)\|_{H^1(B \setminus \bar{D})}$ and hence $\|W(\cdot, z)\|_{L^2(\mathcal{C} \setminus \partial D)}$ is bounded with respect to z near a . In addition, $\|G(\cdot, x)\|_{L^2(\mathcal{C} \setminus \partial D)}$ is bounded with respect to $x \in B \setminus D$ since $G(x, z) = O(\ln(|x - z|))$. Hence $\int_{\mathcal{C} \setminus \partial D} \sigma(y) G(y, x) W(y, z_p) ds(y)$ is bounded for $x \in B \setminus D$ and z_p near a . From (39), we conclude that $W(x, z_p) = O(1)$ for $x, z_p \in B \setminus D$ near a . Rewriting this estimate in the form

$$(H_\sigma - \tilde{H}_\sigma)(x, z_p) = (E^s - \tilde{E}^s)(x, z_p) = O(1)$$

for $x, z_p \in B \setminus D$ near a , we deduce that $\tilde{E}^s(x, z_p)$ is the dominant part of $E^s(x, z_p)$ for x, z_p in $B \setminus D$ near a .

Part two. Analysis of $E^s(x, z)$ near a .

In the next steps, we will analyze $\tilde{E}^s(x, z)$ near the point a . To this end, we introduce $\tilde{E}_{\sigma(a)}^s(\cdot, z_p)$ and $\tilde{E}_{\sigma(a), \Phi}^s(\cdot, z)$ as the solutions to the following two problems

$$\begin{cases} (\Delta + \kappa^2) \tilde{E}_{\sigma(a)}^s(x, z_p) = 0 & \text{in } \mathbb{R}^2 \setminus \bar{D} \\ \left(\frac{\partial}{\partial \nu} + i\kappa\sigma(a)\right) \tilde{E}_{\sigma(a)}^s = -(\partial_\nu + i\sigma(a)) \frac{\partial}{\partial x_2} \Phi(\cdot, z_p) & \text{on } \partial D \\ \tilde{E}_{\sigma(a)}^s(\cdot, z) \text{ satisfies the Sommerfeld radiation condition,} \end{cases} \quad (40)$$

$$\begin{cases} (\Delta + \kappa^2) \tilde{E}_{\sigma(a), \Phi}^s(x, z) = 0 & \text{in } \Omega \setminus \bar{D} \\ \left(\frac{\partial}{\partial \nu} + i\kappa\sigma(a)\right) \tilde{E}_{\sigma(a), \Phi}^s(x, z) = -\left(\frac{\partial}{\partial \nu} + i\kappa\sigma(a)\right) \frac{\partial}{\partial x_2} \Phi(x, z_p) & \text{on } \partial D \\ \tilde{E}_{\sigma(a), \Phi}^s(\cdot, z) = -\frac{\partial}{\partial x_2} \Phi(x, z_p) & \text{on } \partial\Omega, \end{cases} \quad (41)$$

respectively, and $\tilde{E}_{\sigma(a),\Gamma}^s(\cdot, z)$ is the solution of (41) replacing Φ by Γ ($\Gamma(x, z) := \frac{1}{2\pi} \ln \frac{1}{|x-z|}$). Moreover, we define $\tilde{E}_{\sigma(a),\Gamma}^{s,0}$ to be the solution of (41) replacing Φ by Γ and the Helmholtz equation by the Laplace equation simultaneously.

Then we have the following lemmas.

LEMMA 4.1

There exist $\delta(a) > 0$ and $C(R) > 0$ such that $|(\tilde{E}^s - \tilde{E}_{\sigma(a)}^s)(x, z_p)| \leq C(R)$ for $z_p \in B(a, \delta(a)) \cap C_{a,\theta}$ and $x \in (\mathbb{R}^2 \setminus D) \cap B(0, R)$, for any $R > 0$ fixed. \square

LEMMA 4.2

There exists $C > 0$ such that

$$|(\tilde{E}_{\sigma(a)}^s - \tilde{E}_{\sigma(a),\Phi}^s)(x, z)| \leq C, \quad |(\tilde{E}_{\sigma(a),\Phi}^s - \tilde{E}_{\sigma(a),\Gamma}^s)(x, z)| \leq C$$

for $z \in \Omega \setminus D$ near D and $x \in \Omega \setminus D$. \square

LEMMA 4.3

There exists $C > 0$ such that $|(\tilde{E}_{\sigma(a),\Gamma}^s - \tilde{E}_{\sigma(a),\Gamma}^{s,0})(x, z)| \leq C$ for $z \in \Omega \setminus D$ near D and $x \in \Omega \setminus D$. \square

LEMMA 4.4

There exist $C > 0$ and $\delta(a) > 0$ such that

$$|(\tilde{E}_{\sigma(a),\Gamma}^{s,0} - w_{\sigma(a)}^+)(z, z)| \leq C$$

for $z \in B(a, \delta(a)) \cap C_{a,\theta}$. \square

We postpone the proof of these four lemmas to section 4.3.

Part three. End of the proof of Proposition 3.1.

By combining Part one and all the four lemmas of Part two together, we finish the proof of Proposition 3.1. \square

4.2. Proof of Proposition 3.2.

The equalities (30) and (31) of this proposition can be proven by expressing

$$\tilde{w}_{\sigma(a)}^{\pm}(\tilde{x}, \tilde{z}) = (U_+[\tilde{x}_2]\phi_{\pm})(\tilde{x}_1), \quad \tilde{w}_D(\tilde{x}, \tilde{z}) = (U_+[\tilde{x}_2]\psi_{\pm})(\tilde{x}_1)$$

in \mathbb{R}_+^2 with $(U_+[\tilde{x}_2]\phi)(\tilde{x}_1) := \frac{1}{2\pi} \int_{\mathbb{R}} e^{i\tilde{x}_1\xi_1 + \tilde{x}_2|\xi_1|} \hat{\phi}(\xi_1, \tilde{z}) d\xi_1$ and computing the density functions ϕ_{\pm} and ψ_{\pm} from the boundary value problems (27), (28), where $\hat{\phi}$ is the 1-dimensional Fourier transform of ϕ , see [17] for explicit computations.

Let us now justify the expansions (32) and (33). Firstly, let us compute the expression of $w_{\sigma(a)}^+$ by integrating by parts. The formula for $w_{\sigma(a)}^-$ is obtained immediately by replacing $\nu(a)$ by $-\nu(a)$ in the expression of $w_{\sigma(a)}^+$. We recall the notation $\tilde{x} = (\tilde{x}_1, \tilde{x}_2)$, $\tilde{z} = (\tilde{z}_1, \tilde{z}_2)$ and assume that $\tilde{x}_2, \tilde{z}_2 > 0$

and $\tilde{x}_1 = \tilde{z}_1$. From (30) in Proposition 3.2, we obtain

$$\begin{aligned} \tilde{w}_{\sigma(a)}^+(\tilde{x}, \tilde{z}) &= \frac{\nu_2(a)}{4\pi} \int_{\mathbb{R}} e^{-(\tilde{x}_2 + \tilde{z}_2)|\xi_1|} \frac{|\xi_1| + i\kappa\sigma(a)}{|\xi_1| - i\kappa\sigma(a)} d\xi_1 \\ &= \frac{\nu_2(a)}{4\pi} \int_{\mathbb{R}} e^{-(\tilde{x}_2 + \tilde{z}_2)|\xi_1|} d\xi_1 + \frac{\nu_2(a)}{4\pi} \int_{\mathbb{R}} e^{-(\tilde{x}_2 + \tilde{z}_2)|\xi_1|} \frac{2i\kappa\sigma(a)}{|\xi_1| - i\kappa\sigma(a)} d\xi_1 \\ &= \frac{\nu_2(a)}{2\pi(\tilde{x}_2 + \tilde{z}_2)} + \frac{\nu_2(a)}{2\pi} (i\kappa\sigma(a)) \int_{\mathbb{R}} \frac{e^{-(\tilde{x}_2 + \tilde{z}_2)|\xi_1|}}{|\xi_1| - i\kappa\sigma(a)} d\xi_1. \end{aligned} \quad (42)$$

However the last integral is

$$\begin{aligned} \int_{\mathbb{R}} \frac{e^{-(\tilde{x}_2 + \tilde{z}_2)|\xi_1|}}{|\xi_1| - i\kappa\sigma(a)} d\xi_1 &= \int_{\mathbb{R}} \frac{e^{-(\tilde{x}_2 + \tilde{z}_2)|\xi_1|}}{|\xi_1| + \kappa\sigma^i(a) - i\kappa\sigma^r(a)} d\xi_1 \\ &= \int_{\mathbb{R}} e^{-(\tilde{x}_2 + \tilde{z}_2)|\xi_1|} \frac{|\xi_1| + \kappa\sigma^i(a) + i\kappa\sigma^r(a)}{(|\xi_1| + \kappa\sigma^i(a))^2 + (\kappa\sigma^r(a))^2} d\xi_1 \\ &= \int_{\mathbb{R}} e^{-(\tilde{x}_2 + \tilde{z}_2)|\xi_1|} \frac{|\xi_1| + \kappa\sigma^i(a)}{(|\xi_1| + \kappa\sigma^i(a))^2 + (\kappa\sigma^r(a))^2} d\xi_1 + O(1) \\ &= 2 \int_0^\infty e^{-(\tilde{x}_2 + \tilde{z}_2)\xi_1} \frac{\xi_1 + \kappa\sigma^i(a)}{(\xi_1 + \kappa\sigma^i(a))^2 + (\kappa\sigma^r(a))^2} d\xi_1 + O(1) \\ &= 2 \int_{\kappa\sigma^i(a)}^\infty e^{-(\tilde{x}_2 + \tilde{z}_2)(r - \kappa\sigma^i(a))} \frac{r}{r^2 + (\kappa\sigma^r(a))^2} d\xi_1 + O(1) \end{aligned} \quad (43)$$

for \tilde{x}_2 and \tilde{z}_2 near 0. On the other hand, direct computations give

$$\int_{\kappa\sigma^i(a)}^\infty e^{-(\tilde{x}_2 + \tilde{z}_2)r} \frac{r}{r^2 + (\kappa\sigma^r(a))^2} d\xi_1 = -\ln(\tilde{x}_2 + \tilde{z}_2) e^{-(\tilde{x}_2 + \tilde{z}_2)\kappa\sigma^i(a)} + O(1) \quad (44)$$

for \tilde{x}_2 and \tilde{z}_2 near 0. Now, combining (42), (43) and (44) together, we are led to

$$\tilde{w}_{\sigma(a)}^+(x, z) = \frac{\nu_2(a)}{2\pi(\tilde{x}_2 + \tilde{z}_2)} - \frac{i\kappa\sigma(a)\nu_2(a)}{\pi} \ln(\tilde{x}_2 + \tilde{z}_2) + O(1) \quad (45)$$

for \tilde{x}_2 and \tilde{z}_2 near 0. In a similar way, using (31) in Proposition 3.2, we obtain for $\tilde{x}_1 = \tilde{z}_1$ that

$$\tilde{w}_D^+(\tilde{x}, \tilde{z}) = \frac{-\nu_2(a)}{2\pi(\tilde{x}_2 + \tilde{z}_2)} + O(1) \quad (46)$$

for \tilde{x}_2 and \tilde{z}_2 near 0. The proof is complete. \square

4.3. Proof of the auxiliary lemmas

This subsection is devoted to the proof of the four lemmas stated and used in section 4.1.

Proof of Lemma 4.1.

We set $R(x, z) := \tilde{E}_\sigma^s(x, z) - w_{\sigma(a)}^s(x, z)$. Then it satisfies

$$\begin{cases} (\Delta + \kappa^2)R(x, z) = 0 & \text{in } \mathbb{R}^2 \setminus \bar{D} \\ \frac{\partial R(x, z)}{\partial \nu} + i\kappa\sigma(a)R(x, z) = -i\kappa(\sigma(x) - \sigma(a))(\tilde{E}^s(x, z) + \frac{\partial}{\partial x_2}\Phi(x, z)) & \text{on } \partial D \\ R(\cdot, z) \text{ satisfies the Sommerfeld radiation condition.} \end{cases} \quad (47)$$

From (47), we have the representation

$$R(x, z) = - \int_{\partial D} i\kappa(\sigma(y) - \sigma(a))G_{\sigma(a)}(y, x)(\tilde{E}^s + \frac{\partial}{\partial x_2}\Phi)(y, z)ds(y), \text{ for } (x, z) \in \mathbb{R}^2 \setminus \bar{D} \quad (48)$$

where $G_{\sigma(a)}$ is the Green's function associated to the scattering problem (47).

We know that $(\tilde{E}^s + \frac{\partial}{\partial x_2}\Phi)(y, z) = \tilde{H}_\sigma$ has the estimate $|\tilde{H}_\sigma(y, z)| \leq \frac{C}{|y-z|}$, then from (48) and the Hölder regularity of $\sigma(x)$, we deduce that

$$|R(x, z)| \leq c \int_{\partial D} |y - a|^\beta \ln(|y - x|)|z - y|^{-1} ds(y).$$

From the inequality $|y - a| \leq c(\theta)|y - z|$ for $y \in \partial D$ and $z \in C_{a,\theta} \cap B(a, \delta(a))$, we have

$$|R(x, z)| \leq c(\theta)c \int_{\partial D} |y - z|^{\beta-1} \ln |y - x| dy$$

and therefore $|R(x, z)| = O(1)$ for $x \in \mathbb{R}^2 \setminus D$ and $z \in C_{a,\theta} \cap B(0, R)$. \square

Proof of Lemma 4.2 and Lemma 4.3.

They can be proven by similar arguments as those in the proof of Lemma 4.1, so we omit the details.

Proof of Lemma 4.4.

The proof of this lemma is quite long. We divide it into several steps. In the first step, we provide an integral representation of $\tilde{E}_{\sigma(a),\Gamma}^{s,0}$ in the local coordinates after flattening ∂D near the point a . In the second step, we use the Taylor expansion of the local metric, induced from the change of variable F related to local parametrization of ∂D , near the point $F(a)$ and the already obtained integral representation to derive the asymptotic expansion of the image of $\tilde{E}_{\sigma(a),\Gamma}^{s,0}$ (under the mentioned change of variable F). In the last step, we come back to the original coordinates and state the asymptotic expansion of $\tilde{E}_{\sigma(a),\Gamma}^{s,0}$ near a .

Step one. An integral representation near the flattened surface.

Let us recall that $\tilde{E}_{\sigma(a),\Gamma}^{s,0}$ satisfies

$$\begin{cases} \Delta \tilde{E}_{\sigma(a),\Gamma}^{s,0}(x, z) = 0 & \text{in } \Omega \setminus \bar{D} \\ (\frac{\partial}{\partial \nu} + i\kappa\sigma(a))(\tilde{E}_{\sigma(a),\Gamma}^{s,0}(\cdot, z)) = -(\frac{\partial}{\partial \nu} + i\kappa\sigma(a))\frac{\partial}{\partial x_2}\Gamma & \text{on } \partial D \\ \tilde{E}_{\sigma(a),\Gamma}^{s,0}(\cdot, z) = -\frac{\partial}{\partial x_2}\Gamma & \text{on } \partial\Omega. \end{cases} \quad (49)$$

We can assume that $a = (0, 0)$ and $\nu(a) = (0, 1)$ by using the rigid transformation of coordinates $T := R_a(\nu(a)) + M_a$ with which (49) needs to be replaced by

$$\begin{cases} \Delta(\tilde{E}_{\sigma(a),\Gamma}^{s,0} \circ T^T)(x, z) = 0 & \text{in } \Omega \setminus \bar{D} \\ (\frac{\partial}{\partial \nu} + i\kappa\sigma(a))(\tilde{E}_{\sigma(a),\Gamma}^{s,0} \circ T^T)(\cdot, z) = -(\frac{\partial}{\partial \nu} + i\kappa\sigma(a))(\nabla\Gamma \cdot \tau_2) & \text{on } \partial D \\ (\tilde{E}_{\sigma(a),\Gamma}^{s,0} \circ T^T)(\cdot, z) = -\nabla\Gamma \cdot \tau_2 & \text{on } \partial\Omega, \end{cases} \quad (50)$$

where $\tau_2 := \tau_2^+ := R_a^+ \begin{bmatrix} 0 \\ 1 \end{bmatrix} = (-\nu_1(a), \nu_2(a))$.

REMARK 4.5

For $a \in \mathcal{C}^-$, we need to replace, in (50), $\tau_2 = \tau_2^+$ by $\tau_2^- := R_a^- \begin{bmatrix} 0 \\ 1 \end{bmatrix} = -R_a^+ \begin{bmatrix} 0 \\ 1 \end{bmatrix} = -\tau_2^+ = -\tau_2$.

Let $\xi = F(x)$ be the local change of variables

$$\xi_1 = x_1, \quad \xi_2 = x_2 - f_a(x_1), \quad (51)$$

where f_a is defined in (18).

Let x, z be points near a . From (50), we deduce that $w(\xi, \eta) = \tilde{E}_{\sigma(a), \Gamma}^{s, 0} \circ T^T(x, z)$ satisfies

$$\begin{cases} \nabla_\xi \cdot B(\xi) \nabla_\xi w(\xi, \eta) = 0, \\ B \nabla_\xi w \cdot \tilde{\nu} + i\kappa\sigma(a) |J^T \tilde{\nu}| w = -\nabla_x (\nabla \Gamma \cdot \tau_2)(F^{-1}(\xi), F^{-1}(\eta)) \cdot J^T \tilde{\nu}(\xi) \\ -i\kappa\sigma(a) |J^T \tilde{\nu}(\xi)| (\nabla \Gamma \cdot \tau_2)(F^{-1}(\xi), F^{-1}(\eta)), \end{cases} \quad (52)$$

where $\xi := F(x)$, $\eta := F(z)$, $B := JJ^T$, $J := \frac{\partial \xi}{\partial x}(F^{-1}(\xi))$ and $\tilde{\nu} := (0, 1)$ is the unit normal to $\partial \mathbb{R}_+^2$. We set $\tilde{R}(\xi, \eta) := w(\xi, \eta) - w_{\sigma(a)}^+(\xi, \eta)$. Then the function $\tilde{R}(\cdot, \eta)$ satisfies

$$\begin{cases} \nabla_\xi \cdot B(\xi) \nabla_\xi \tilde{R} = \nabla_\xi \cdot (I - B) \nabla_\xi \omega_{\sigma(a)}^+, \\ B(\xi) \nabla_\xi \tilde{R} \cdot \tilde{\nu} + i\kappa\sigma(a) |J^T \tilde{\nu}(\xi)| \tilde{R} = (I - B) \nabla_\xi \omega_{\sigma(a)}^+ \cdot \tilde{\nu}(\xi) + \\ i\kappa\sigma(a) [(1 - |J^T \tilde{\nu}(\xi)|) w_{\sigma(a)}^+ + (\nabla \Gamma \cdot \tau_2)(\xi, \eta) - |J^T \tilde{\nu}(\xi)| (\nabla \Gamma \cdot \tau_2) \circ F^{-1}(\xi, \eta)) \\ + \nabla_x (\nabla \cdot \tau_2)(\xi, \eta) \cdot \tilde{\nu}(\xi) - \nabla_x (\nabla \cdot \tau_2) \circ F^{-1}(\xi, \eta) |J^T \tilde{\nu}(\xi)|, \end{cases} \quad (53)$$

where the first relation holds in \mathbb{R}_+^2 near $F(a)$, while the second one is satisfied on $\partial \mathbb{R}_+^2$ near $F(a)$. Since we assumed $a = (0, 0)$, then we have also $F(a) = (0, 0)$. In (53), we abused a little bit the notation by setting $F^{-1}(\xi, \eta) := (F^{-1}(\xi), F^{-1}(\eta))$.

We take $B(0, r)$ to be the circle of center 0 and radius r and set $B_r^+ := B(0, r) \cap \mathbb{R}_+^2$. Let us also divide the boundary ∂B_r^+ of B_r^+ as follows $\partial B_r^+ = S_r \cup S_r^c$ with $S_r := \partial B_r^+ \cap \partial F(D)$.

We denote by G the Green's function satisfying:

$$\begin{cases} \nabla_\xi \cdot B(\xi) \nabla_\xi G(\xi, \eta) = -\delta(\xi, \eta), \text{ in } B_r^+(0, r), \\ B(\xi) \nabla G(\xi, \eta) \cdot \nu(\xi) + i\sigma(a) |J^T \tilde{\nu}(\xi)| G(\xi, \eta) = 0 \text{ on } \partial B_r^+(0, r), \end{cases} \quad (54)$$

where ν is the outward unit normal on ∂B_r^+ and $|J^T \tilde{\nu}(\xi)| = \sqrt{1 + (f'_a(\xi_1))^2}$ on S_r and extended smoothly to S_r^c . This Green's function G is to be distinguished from the one used in **Part One** of section 4.1.

Integrating by parts in (53), using G , generates the following integral representation of $\tilde{R}(\xi, \eta)$:

$$\begin{aligned} \tilde{R}(\xi, \eta) &= \int_{B_r^+} (I - B) \nabla G(z, \xi) \cdot \nabla \omega_{\sigma(a)}^+(z, \eta) dz + \\ &\quad i\kappa\sigma(a) \left\{ \int_{S_r} [1 - |J^T \tilde{\nu}(z)|] w^+(z, \eta) G(z, \xi) ds(z) + \right. \\ &\quad \int_{S_r} [\nabla \Gamma \cdot \tau_2(z, \eta) - |J^T \tilde{\nu}(z)| \nabla \Gamma \cdot \tau_2(F^{-1}(z), F^{-1}(\eta))] G(z, \xi) ds(z) - \\ &\quad \left. \int_{S_r} [\nabla_z (\nabla \Gamma \cdot \tau_2)(z, \eta) \cdot \tilde{\nu}(z) - \nabla_z (\nabla \Gamma \cdot \tau_2)(F^{-1}(z), F^{-1}(\eta)) \cdot J^T \tilde{\nu}(z)] G(z, \xi) ds(z) \right\} \\ &\quad + O(1). \end{aligned} \quad (55)$$

for ξ, η near $F(a)$. Notice that $\tilde{\nu}$ is oriented towards the interior of B_r^+ , since it is defined to be oriented into the exterior of D . In addition, $\tilde{\nu} = (0, 1)$ on S_r , i.e. S_r is flat. The term $O(1)$ represents the total of the surface integrals over S_r^c since ξ and η are away from S_r^c .

Step two. The estimate of $\tilde{R}(\xi, \eta)$ near $F(a)$. We need the following lemma on some precise estimates of the Green's function G .

LEMMA 4.6

Let $x \in B_r^+$ and $z \in C_{F(a),\theta}$ small enough, then

$$G(x, z) = \Gamma(x, z) + \Gamma(x, z^*) + O(1) \tag{56}$$

and

$$\frac{\partial}{\partial x_j} G(x, z) = \frac{\partial}{\partial x_j} \Gamma(x, z) + \frac{\partial}{\partial x_j} \Gamma(x, z^*) + \frac{O(z_1)}{|x - z|} + O(\ln(x_2)), \quad j = 1, 2 \tag{57}$$

for $|x - z| \rightarrow 0$, where $z^* = (z_1, -z_2)$. □

REMARK 4.7

It is well known that we have the following rough estimates of G , see for instance [19, 20]:

$$|G(x, z)| \leq c |\ln(|x - z|)| \text{ and } |\nabla G(x, z)| \leq c |x - z|^{-1}.$$

The goal of this lemma is to give a more precise and explicit behavior of G and its derivatives. Remark that the term $\frac{O(z_1)}{|x - z|}$ is related to the matrix B . This term vanishes if $B = I$. The term $O(\ln(x_2))$ is related to the existence of the surface impedance. It also vanishes if $\sigma = 0$. The logarithm appears also for the flattened surfaces, see Proposition 3.2. □

Proof of Lemma 4.6.

We set $\Gamma_F(x, z) := \Gamma(F^{-1}(x), F^{-1}(z)) + \Gamma(F^{-1}(x), F^{-1}(z^*))$. It is clear that $\nabla_x \cdot B \nabla_x \Gamma_F(x, z) = -\delta(x, z) - \delta(x, z^*)$ in \mathbb{R}^2 . Hence $G - \Gamma_F$ satisfies

$$\begin{cases} \nabla_x \cdot B(x) \nabla_x (G - \Gamma_F)(x, z) = 0, \text{ in } B_r^+ \\ B(x) \nabla_x (G - \Gamma_F)(x, z) \cdot \nu + i\kappa\sigma(a) |J^T \tilde{\nu}| (G - \Gamma_F) = \\ -B(x) \nabla_x \Gamma_F \cdot \nu + i\kappa\sigma(a) |J^T \tilde{\nu}| \Gamma_F \text{ on } \partial B_r^+. \end{cases} \tag{58}$$

An integration by parts gives:

$$(G - \Gamma_F)(x, z) = - \int_{\partial B_r^+} B(t) \nabla_t \Gamma_F(t, z) \cdot \nu(t) G(t, x) ds(t) - i\kappa\sigma(a) \int_{\partial B_r^+} |J^T \tilde{\nu}| \Gamma_F(t, z) G(t, x) ds(t)$$

which we write as

$$\begin{aligned} (G - \Gamma_F)(x, z) = & - \int_{S_r} (I - B) \nabla \Gamma_F(t, z) \cdot \nu(t) G(t, x) ds(t) - \int_{S_r^c} (I - B) \nabla \Gamma_F(t, z) \cdot \nu(t) G(t, x) ds(t) + \\ & \int_{S_r} \frac{\partial}{\partial t_2} \Gamma_F(t, z) G(t, x) dt_2 + \int_{S_r^c} \nabla \Gamma_F(t, z) \cdot \nu(t) G(t, x) ds(t) - \\ & i\kappa\sigma(a) \int_{S_r} |J^T \tilde{\nu}| \Gamma_F(t, z) G(t, x) dt - i\kappa\sigma(a) \int_{S_r^c} |J^T \tilde{\nu}| \Gamma_F(t, z) G(t, x) dt. \end{aligned} \tag{59}$$

Since we are interested by z in $C_{a,\theta}$ near the point a , then the integrals over S_r^c and their derivatives are bounded with respect to x and z . Hence, we will consider only the integrals over S_r .

Recall that $\Gamma(x, z) := \frac{1}{2\pi} \ln\left(\frac{1}{|x-z|}\right)$, then

$$\left(\frac{\partial}{\partial x_1}\Gamma\right)(F^{-1}(x), F^{-1}(z)) = -\frac{1}{2\pi} \frac{x_1 - z_1}{|F^{-1}(x) - F^{-1}(z)|^2}$$

and

$$\left(\frac{\partial}{\partial x_2}\Gamma\right)(F^{-1}(x), F^{-1}(z)) = -\frac{1}{2\pi} \frac{x_2 - z_2 - f_a(x_1) - f_a(z_1)}{|F^{-1}(x) - F^{-1}(z)|^2}.$$

Let us estimate the term $|F^{-1}(x) - F^{-1}(z)|^{-2}$. From (51), we obtain

$$\begin{aligned} |F^{-1}(x) - F^{-1}(z)|^2 &= (x_1 - z_1)^2 + [x_2 - z_2 + f_a(x_1) - f_a(z_1)]^2 \\ &= |x - z|^2 + 2(x_2 - z_2)[f_a(x_1) - f_a(z_1)] + [f_a(x_1) - f_a(z_1)]^2. \end{aligned}$$

Expanding $f_a(x_1)$ to the order two near the point z_1 , recalling that $f_a \in C^3(-r, r)$, we obtain:

$$f_a(x_1) - f_a(z_1) = f'_a(z_1)(x_1 - z_1) + \frac{1}{2}f''_a(z_1)(x_1 - z_1)^2 + O((x_1 - z_1)^3).$$

Hence, we can write:

$$|F^{-1}(x) - F^{-1}(z)|^2 = |x - z|^2 \left\{ 1 + 2f'_a(z_1) \frac{(x_1 - z_1)(x_2 - z_2)}{|x - z|^2} + (f'_a(z_1))^2 \frac{(x_1 - z_1)^2}{|x - z|^2} + O(|x - z|) \right\}.$$

Taking z small enough and using the property $f'_a(z_1) = O(z_1)$, we can write

$$1 + 2f'_a(z_1) \frac{(x_1 - z_1)(x_2 - z_2)}{|x - z|^2} + (f'_a(z_1))^2 \frac{(x_1 - z_1)^2}{|x - z|^2} = 1 + O(z_1).$$

Taking, in addition, $|x - z|$ small enough, we obtain:

$$|F^{-1}(x) - F^{-1}(z)|^{-2} = \frac{1 + O(z_1) + O(|x - z|)}{|x - z|^2}. \quad (60)$$

This estimate implies that:

$$\left(\frac{\partial}{\partial x_1}\Gamma\right)(F^{-1}(x), F^{-1}(z)) = -\frac{1}{2\pi} \frac{x_1 - z_1}{|x - z|^2} + \frac{O(z_1)}{|x - z|} + O(1) \quad (61)$$

and

$$\left(\frac{\partial}{\partial x_2}\Gamma\right)(F^{-1}(x), F^{-1}(z)) = -\frac{1}{2\pi} \frac{x_2 - z_2}{|x - z|^2} + \frac{O(z_1)}{|x - z|} + O(1). \quad (62)$$

From the chain rule $\nabla\Gamma_F(x, z) = (J^T(x)\nabla\Gamma)(F^{-1}(x), F^{-1}(z))$ and the properties of J , we obtain:

$$\frac{\partial}{\partial x_1}(\Gamma(F^{-1}(x), F^{-1}(z))) = -\frac{1}{2\pi} \frac{x_1 - z_1}{|x - z|^2} + \frac{O(z_1)}{|x - z|} + O(1) \quad (63)$$

and

$$\frac{\partial}{\partial x_2}(\Gamma(F^{-1}(x), F^{-1}(z))) = -\frac{1}{2\pi} \frac{x_2 - z_2}{|x - z|^2} + \frac{O(z_1)}{|x - z|} + O(1). \tag{64}$$

In addition, it is easy to see from (60) that:

$$\Gamma(F^{-1}(x), F^{-1}(z)) = -\frac{1}{2\pi} \ln|x - z| + O(1) = \Gamma(x, z) + O(1). \tag{65}$$

The identity (64) implies that $\frac{\partial}{\partial t_2} \Gamma_F(t, z) = \frac{O(z_1)}{|t - z|} + O(1)$ on S_r . Hence, we obtain from (59):

$$\begin{aligned} |(G - \Gamma_F)(x, z)| \leq \\ c_1 \int_{S_r} |t_1| \frac{\ln(|t - x|)}{|t - z|} dt_1 + c_2 |z_1| \int_{S_r} \frac{|\ln(|t - x|)|}{|t - z|} dt_1 + c_3 \int_{S_r} |\ln(|t - z|)| |\ln(|t - x|)| dt_1 \end{aligned}$$

with positive constants c_1, c_2 and c_3 . Then

$$|(G - \Gamma_F)(x, z)| = O\left(\frac{|z_1|}{|z_2|}\right) = O(1), \text{ for } z \in C_{a,\theta}. \tag{66}$$

In addition, differentiating in (59), for $j = 1, 2$, we have the estimate:

$$\left| \frac{\partial}{\partial x_j} (G - \Gamma_F)(x, z) \right| \leq c_1 \int_{S_r} |t_1| \frac{1}{|t - x||t - z|} dt_1 + c_2 |z_2| \int_{S_r} \frac{1}{|t - x||t - z|} dt_1 + c_3 \int_{S_r} \frac{1}{|t - x|} dt_1$$

which implies that

$$\left| \frac{\partial}{\partial x_j} (G - \Gamma_F)(x, z) \right| = O(\ln(x_2)), \text{ for } z \in C_{a,\theta}. \tag{67}$$

Finally from (65)-(66) and (63)-(64)-(67), we obtain the estimates of Lemma 4.6. \square

Step two continued.

Due to the form of $w_{\sigma(a)}^+$, see Proposition 3.2, we have $w_{\sigma(a)}^+(z, \eta) = \nabla \Gamma(z, \eta^*) \cdot \tau_2 + O(\ln(|z_2 + \eta_2|))$. Since $J^T \tilde{\nu}(z) = (-f'_a(z_1), 1)$ then $|1 - |J^T \tilde{\nu}(z)|| \leq \frac{1}{2}(f'_a(z_1))^2$. With this inequality, we deduce that the second term of (55) is bounded for $\xi = \eta, \eta \in C_{F(a),\theta}$.

The next step is to prove that

$$\int_{B_r^+} (I - B) \nabla G(z, \xi) \cdot \nabla \omega_{\sigma(a)}^+(z, \eta) dz = O(1), \tag{68}$$

$$\int_{S_r} [\nabla \Gamma \cdot \tau_2(z, \eta) - |J^T \tilde{\nu}(z)| \nabla \Gamma \cdot \tau_2(F^{-1}(z), F^{-1}(\eta))] G(z, \xi) ds(z) = O(1) \tag{69}$$

and

$$\int_{S_r} [\nabla_z (\nabla \Gamma \cdot \tau_2)(z, \eta) \cdot \tilde{\nu}(z) - \nabla_z (\nabla \Gamma \cdot \tau_2)(F^{-1}(z), F^{-1}(\eta)) \cdot J^T \tilde{\nu}(z)] G(z, \xi) ds(z) = O(1) \tag{70}$$

for $\xi = \eta$ with $\eta \in C_{F(a),\theta}$.

As we will do it next, using Lemma 4.6, it is enough to prove (68), (69) and (70) replacing $G(x, z)$ by $\Gamma(x, z) + \Gamma(x, z^*)$ and $w_{\sigma(a)}^+(x, z)$ by $\Gamma(x, z^*)$.

Proof of (68).

To this end, we use the explicit form of B , i.e.

$$B(z) := \begin{bmatrix} 1 & -f'_a(z_1) \\ -f'_a(z_1) & 1 + (f'_a)^2(z_1) \end{bmatrix}$$

to write the Taylor expansion

$$B(z) - B(\eta) = \begin{bmatrix} 0 & -f''_a(\eta_1)(z_1 - \eta_1) \\ -f''_a(\eta_1)(z_1 - \eta_1) & 2f'_a(\eta_1)f''_a(\eta_1)(z_1 - \eta_1) \end{bmatrix} + O(|z_1 - \eta_1|^2) \text{ for } z \text{ near } \eta$$

and then we obtain the expansion

$$B(z) - B(\eta) = \begin{bmatrix} 0 & -1 \\ -1 & 0 \end{bmatrix} f''_a(\eta_1)(z_1 - \eta_1) + O(\eta_1)O(z_1 - \eta_1) + O(|z_1 - \eta_1|^2) \text{ for } z \text{ near } \eta.$$

Using the notation $\partial z_j := \frac{\partial}{\partial z_j}$, we write

$$\begin{aligned} & \int_{B_r^+} (B(\eta) - B(z)) \nabla G(z, \xi) \cdot \nabla \Gamma_{\sigma(a)}(z, \eta) dz = \\ & f''_a(\eta_1) \int_{B_r^+} (z_1 - \eta_1) [\partial_{z_2} G(z, \xi) \partial_{z_1} (\partial_{z_2} \Gamma_{\sigma(a)})(z, \eta) + \partial_{z_1} G(z, \xi) \partial_{z_2} (\partial_{z_2} \Gamma_{\sigma(a)})(z, \eta)] dz + \\ & O(1). \end{aligned} \tag{71}$$

Again from the property

$$\omega_{\sigma(a)}^+(z, \eta) = \nabla \Gamma(z, \eta^*) \cdot \tau_2 + O(\ln |\eta_2|) \text{ for } z \text{ near } \eta$$

and (56)-(57), it is enough to compute the integrals of (71) for $\Gamma(z, \xi)$ and $\partial_{z_j} \Gamma(z, \eta^*)$. Hence we have

$$\begin{aligned} & \int_{B_r^+} (B(\eta) - B(z)) \nabla G(z, \xi) \cdot \nabla \omega_{\sigma(a)}^+(z, \eta) dz \\ &= 2f''_a(\eta_1) \int_{B_r^+} (z_1 - \eta_1) \left[\frac{\partial \Gamma}{\partial z_2}(z, \xi) \frac{\partial}{\partial z_1} (\nabla \Gamma)(z, \eta^*) \cdot \tau_2 + \frac{\partial \Gamma}{\partial z_1}(z, \xi) \frac{\partial}{\partial z_2} (\nabla \Gamma)(z, \eta^*) \cdot \tau_2 \right] dz + O(1) \\ &= 2f''_a(\eta_1) [-\nu_1(a)] \int_{B_r^+} (z_1 - \eta_1) \left[\frac{\partial \Gamma}{\partial z_2}(z, \xi) \frac{\partial}{\partial z_1} \left(\frac{\partial}{\partial z_1} \Gamma \right)(z, \eta^*) + \frac{\partial \Gamma}{\partial z_1}(z, \xi) \frac{\partial}{\partial z_2} \left(\frac{\partial \Gamma}{\partial z_1} \right)(z, \eta^*) \right] dz + \\ & 2f''_a(\eta_1) \nu_2(a) \int_{B_r^+} (z_1 - \eta_1) \left[\frac{\partial \Gamma}{\partial z_2}(z, \xi) \frac{\partial}{\partial z_1} \left(\frac{\partial}{\partial z_2} \Gamma \right)(z, \eta^*) + \frac{\partial \Gamma}{\partial z_1}(z, \xi) \frac{\partial}{\partial z_2} \left(\frac{\partial \Gamma}{\partial z_2} \right)(z, \eta^*) \right] dz + O(1). \end{aligned} \tag{72}$$

We start by the first integral in (72). We have:

$$\begin{aligned} & \frac{\partial \Gamma}{\partial z_2}(z, \xi) \frac{\partial}{\partial z_1} \left(\frac{\partial \Gamma}{\partial z_1} \right)(z, \eta^*) + \frac{\partial \Gamma}{\partial z_1}(z, \xi) \frac{\partial}{\partial z_2} \left(\frac{\partial \Gamma}{\partial z_1} \right)(z, \eta^*) \\ &= \frac{1}{4\pi^2} \left[\frac{(z - \xi) \cdot (0, 1)}{|z - \xi|^2} \left[\frac{1}{|z - \eta^*|^2} - 2 \frac{[(z - \eta^*) \cdot (1, 0)]^2}{|z - \eta^*|^4} \right] - \right. \\ & \left. 2 \frac{(z - \xi) \cdot (1, 0)}{|z - \xi|^2} \left[(z - \eta^*) \cdot (1, 0) \frac{(z - \eta^*) \cdot (0, 1)}{|z - \eta^*|^4} \right] \right]. \end{aligned} \tag{73}$$

Hence

$$\begin{aligned} & (z_1 - \eta_1) \left[\frac{\partial \Gamma}{\partial z_2}(z, \xi) \frac{\partial}{\partial z_1} \left(\frac{\partial \Gamma}{\partial z_1} \right)(z, \eta^*) + \frac{\partial \Gamma}{\partial z_1}(z, \xi) \frac{\partial}{\partial z_2} \left(\frac{\partial \Gamma}{\partial z_1} \right)(z, \eta^*) \right] \\ = & \frac{1}{4\pi^2} \left[\frac{(z_1 - \eta_1)(z_2 - \xi_2)}{|z - \xi|^2 |z - \eta^*|^2} - 2 \frac{(z_1 - \eta_1)^3 (z_2 - \xi_2)}{|z - \xi|^2 |z - \eta^*|^4} - 2 \frac{(z_1 - \eta_1)^2 (z_1 - \xi_1)(z_2 + \eta_2)}{|z - \xi|^2 |z - \eta^*|^4} \right]. \end{aligned}$$

Since in the limit case, i.e. $\xi = \eta = 0$, this function is anti-symmetric in any rectangle of B_r^+ , then we show that the first integral in (72) is bounded for $\xi = \eta$, $\xi \in C_{F(a), \theta}$, near $F(a)$.

Let us compute the second integral of (72). We have:

$$\begin{aligned} & \frac{\partial \Gamma}{\partial z_2}(z, \xi) \frac{\partial}{\partial z_1} \left(\frac{\partial \Gamma}{\partial z_2} \right)(z, \eta^*) + \frac{\partial \Gamma}{\partial z_1}(z, \xi) \frac{\partial}{\partial z_2} \left(\frac{\partial \Gamma}{\partial z_2} \right)(z, \eta^*) \\ = & \frac{1}{4\pi^2} \left[-2 \frac{(z - \xi) \cdot (0, 1)}{|z - \xi|^2} (z - \eta^*) \cdot (0, 1) \frac{(z - \eta^*) \cdot (1, 0)}{|z - \eta^*|^4} + \right. \\ & \left. \frac{(z - \xi) \cdot (1, 0)}{|z - \xi|^2} \left(\frac{1}{|z - \eta^*|^2} - 2 \frac{[(z - \eta^*) \cdot (0, 1)]^2}{|z - \eta^*|^4} \right) \right]. \end{aligned} \tag{74}$$

In contrast to the integrand of the first integral in (72), related to (73), the integrand of the second integral, related to (74), is not anti-symmetric (but actually symmetric) in the limit case, i.e. $\xi = \eta$, in B_r^+ . Hence we need to compute explicitly this integral. We write (74) as

$$\frac{\partial \Gamma}{\partial z_2}(z, \xi) \frac{\partial}{\partial z_1} \left(\frac{\partial \Gamma}{\partial z_2} \right)(z, \eta^*) + \frac{\partial \Gamma}{\partial z_1}(z, \xi) \frac{\partial}{\partial z_2} \left(\frac{\partial \Gamma}{\partial z_2} \right)(z, \eta^*) = -\frac{1}{4\pi^2} [-I + II - III],$$

where we set

$$I := 2 \frac{(z_2 - \xi_2)(z_2 + \eta_2)(z_1 - \eta_1)}{|z - \xi|^2 |z - \eta^*|^4}, \quad II := \frac{z_1 - \xi_1}{|z - \xi|^2 |z - \eta^*|^2}, \quad III := 2 \frac{(z_2 + \eta_2)^2 (z_1 - \xi_1)}{|z - \xi|^2 |z - \eta^*|^4}.$$

In the following, we estimate the integrals related to I, II and III.

Let us estimate the integral related to I:

$$\int_{B_r^+} 2(z_1 - \eta_1) \frac{(z_2 - \xi_2)(z_2 + \eta_2)(z_1 - \eta_1)}{|z - \xi|^2 |z - \eta^*|^4} dz.$$

Let $r_1 > 0$ and $r_2 > 0$ be such that $(-r_1, r_1) \times (0, r_2) \subset B_r^+$. Since we are interested in $\xi \in S_r$ and $\eta \in C_{F(a), \theta}$, then

$$\begin{aligned} & \int_{B_r^+} 2(z_1 - \eta_1) \frac{(z_2 - \xi_2)(z_2 + \eta_2)(z_1 - \eta_1)}{|z - \xi|^2 |z - \eta^*|^4} dz \\ = & \int_0^{r_2} \int_{-r_1}^{r_1} 2(z_1 - \eta_1) \frac{(z_2 - \xi_2)(z_2 + \eta_2)(z_1 - \eta_1)}{|z - \xi|^2 |z - \eta^*|^4} dz_1 dz_2 + O(1). \end{aligned}$$

Hence we can write

$$\begin{aligned} & \int_{B_r^+} (z_1 - \eta_1) \frac{(z_2 - \xi_2)(z_2 + \eta_2)(z_1 - \eta_1)}{|z - \xi|^2 |z - \eta^*|^4} dz \\ = & \int_0^{r_2} (z_2 - \xi_2)(z_2 + \eta_2) \left[\int_{-r_1}^{r_1} \frac{(z_1 - \eta_1)^2}{|z - \xi|^2 |z - \eta^*|^4} dz_1 \right] dz_2 + O(1) \end{aligned} \tag{75}$$

for ξ, η near $F(a)$. However

$$\begin{aligned} & \int_{-r_1}^{r_1} \frac{(z_1 - \eta_1)^2}{|z - \xi|^2 |z - \eta^*|^4} dz_1 = \int_{-r_1}^{r_1} \frac{(z_1 - \eta_1)^2 |z - \eta^*|^2}{|z - \xi|^2 |z - \eta^*|^6} dz_1 \\ &= \int_{-r_1}^{r_1} \frac{(z_1 - \eta_1)^2 |z - \xi|^2}{|z - \xi|^2 |z - \eta^*|^6} dz_1 + \int_{-r_1}^{r_1} \frac{(z_1 - \eta_1)^2 [|\xi - \eta^*|^2 + 2(\xi - \eta^*) \cdot (z - \xi)]}{|z - \xi|^2 |z - \eta^*|^6} dz_1. \end{aligned}$$

Remark that

$$\begin{aligned} & \left| \int_0^{r_2} \int_{-r_1}^{r_1} \frac{(z_2 - \xi_2)(z_2 + \eta_2)(z_1 - \eta_1)^2 [|\xi - \eta^*|^2 + 2(\xi - \eta^*) \cdot (z - \xi)]}{|z - \xi|^2 |z - \eta^*|^6} dz_1 dz_2 \right| \\ & \leq \int_0^{r_2} \int_{-r_1}^{r_1} \left[\frac{|\xi - \eta^*|^2}{|z - \xi| |z - \eta^*|^3} + 2 \frac{|\xi - \eta^*|}{|z - \eta^*|^3} \right] dz_1 dz_2 = O\left(\frac{|\xi - \eta^*|^2}{\eta_2^2}\right) + O\left(\frac{|\xi - \eta^*|}{\eta_2}\right), \end{aligned}$$

which is bounded for $\xi = \eta$. Now we have

$$\int_{-r_1}^{r_1} \frac{(z_1 - \eta_1)^2}{|z - \eta^*|^6} dz_1 = \int_{-r_1}^{r_1} \frac{1}{|z - \eta^*|^4} dz_1 - (z_2 + \eta_2)^2 \int_{-r_1}^{r_1} \frac{1}{|z - \eta^*|^6} dz_1.$$

We obtain after a change of variables

$$\int_{-r_1}^{r_1} \frac{1}{|z - \eta^*|^4} dz_1 = \frac{1}{|z_2 + \eta_2|^3} \int_{\arctan \frac{-r_1 - \eta_1}{|z_2 + \eta_2|}}^{\arctan \frac{r_1 - \eta_1}{|z_2 + \eta_2|}} \cos^2 \theta d\theta,$$

and similarly

$$\int_{-r_1}^{r_1} \frac{1}{|z - \eta^*|^6} dz_1 = \frac{1}{|z_2 + \eta_2|^5} \int_{\arctan \frac{-r_1 - \eta_1}{|z_2 + \eta_2|}}^{\arctan \frac{r_1 - \eta_1}{|z_2 + \eta_2|}} \cos^4 \theta d\theta.$$

We use the formula $\cos^4 \theta = \cos^2 \theta - \frac{1}{8} + \frac{1}{8} \cos(4\theta)$ to obtain

$$\begin{aligned} \int_{-r_1}^{r_1} \frac{(z_1 - \eta_1)^2}{|z - \eta^*|^6} dz_1 &= \frac{1}{8|z_2 + \eta_2|^3} \left[\arctan \frac{r_1 - \eta_1}{|z_2 + \eta_2|} - \arctan \frac{-r_1 - \eta_1}{|z_2 + \eta_2|} \right] - \\ & \quad \frac{1}{4} \left[\sin 4\left(\arctan \frac{r_1 - \eta_1}{|z_2 + \eta_2|}\right) - \sin 4\left(\arctan \frac{-r_1 - \eta_1}{|z_2 + \eta_2|}\right) \right]. \end{aligned}$$

Inserting this last equality in (75) for $\xi = \eta$, we have

$$\begin{aligned} & \int_{B_r^+} (z_1 - \eta_1) \frac{(z_2 + \xi_2)(z_2 + \eta_2)(z_1 - \eta_1)}{|z - \xi|^2 |z - \eta^*|^4} dz \\ &= \int_0^{r_2} \frac{1}{8|z_2 + \eta_2|} \left[\arctan \frac{r_1 - \eta_1}{|z_2 + \eta_2|} - \arctan \frac{-r_1 - \eta_1}{|z_2 + \eta_2|} \right] dz_2 - \\ & \quad \int_0^{r_2} \frac{1}{32|z_2 + \eta_2|} \left[\sin 4\left(\arctan \frac{r_1 - \eta_1}{|z_2 + \eta_2|}\right) - \sin 4\left(\arctan \frac{-r_1 - \eta_1}{|z_2 + \eta_2|}\right) \right] dz_2 + O(1). \end{aligned}$$

Hence, we get the estimate

$$\int_{B_r^+} (z_1 - \eta_1) \frac{(z_2 - \xi_2)(z_2 + \eta_2)(z_1 - \eta_1)}{|z - \xi|^2 |z - \eta^*|^4} dz = -\frac{\pi}{8} \ln \eta_2 + O(1)$$

for $\xi = \eta$ and $\eta \in C_{F(a),\theta}$ near $F(a)$. Similar computations give the following estimates of the integrals of II and III:

$$\int_{B_r^+} \frac{(z_2 - \xi_2)(z_2 + \eta_2)(z_1 - \eta_1)(z_1 - \xi_1)}{|z - \xi|^2 |z - \eta^*|^4} dz = -\frac{\pi}{8} \ln \eta_2 + O(1)$$

and

$$\int_{B_r^+} \frac{(z_1 - \xi_1)(z_1 - \eta_1)}{|z - \xi|^2 |z - \eta^*|^2} dz = -\frac{\pi}{2} \ln \eta_2 + O(1)$$

for $\xi = \eta$ with $\eta \in C_{F(a),\theta}$ near $F(a)$. Then replacing these values in (72) by using (73) yields

$$\int_{B_r^+} (B(z) - B(\eta)) \nabla G(z, \xi) \cdot \nabla w_{\sigma(a)}^+(z, \eta) dz = O(1)$$

for $\xi = \eta$ with $\eta \in C_{F(a),\theta}$ near $F(a)$.

Now, using the estimate

$$\left| \int_{B_r^+} (I - B(\eta)) \nabla G(z, \xi) \cdot \nabla w_{\sigma(a)}^+(z, \eta^*) dz \right| \leq C |\eta| \int_{B_r^+} \frac{1}{|z - \xi|} \frac{1}{|z - \eta^*|^2} dz,$$

we conclude that

$$\int_{B_r^+} (I - B(z)) \nabla G(z, \xi) \cdot \nabla w_{\sigma(a)}^+(z, \eta^*) dz = O(1)$$

for $\xi, \eta \in C_{F(a),\theta}$ and $\xi = \eta$ near $F(a)$.

Proof of (69).

Let us now consider the surface integral

$$\int_{S_r} [(\nabla \Gamma \cdot \tau_2)(z, \eta) - |J^T \tilde{\nu}| (\nabla \Gamma \cdot \tau_2)(F^{-1}(z), F^{-1}(\eta))] G(z, \eta) dz_1.$$

We separate it into two parts as follows:

$$\begin{aligned} & \int_{S_r} [(\nabla \Gamma \cdot \tau_2)(z, \eta) - (\nabla \Gamma \cdot \tau_2)(F^{-1}(z), F^{-1}(\eta))] G(z, \eta) dz_1 + \\ & \int_{S_r} [1 - |J^T \tilde{\nu}|] (\nabla \Gamma \cdot \tau_2)(F^{-1}(z), F^{-1}(\eta))] G(z, \eta) dz_1. \end{aligned}$$

We start by estimating the first term: $\int_{S_r} [(\nabla \Gamma \cdot \tau_2)(z, \eta) - (\nabla \Gamma \cdot \tau_2)(F^{-1}(z), F^{-1}(\eta))] G(z, \eta) dz_1$.

Using (61) and (62), we obtain

$$(\nabla \Gamma \cdot \tau_2)(z, \eta) - (\nabla \Gamma \cdot \tau_2)(F^{-1}(z), F^{-1}(\eta)) = \frac{O(\eta_1)}{|z - \eta|} + O(1),$$

hence:

$$\int_{S_r} [(\nabla \Gamma \cdot \tau_2)(z, \eta) - (\nabla \Gamma \cdot \tau_2)(F^{-1}(z), F^{-1}(\eta))] G(z, \eta) dz_1 = O(\eta_1) \int_{S_r} \frac{\ln(|z - \eta|)}{|z - \eta|} dz_1 + O(1),$$

which means that

$$\int_{S_r} [(\nabla\Gamma \cdot \tau_2)(z, \eta) - (\nabla\Gamma \cdot \tau_2)(F^{-1}(z), F^{-1}(\eta))]G(z, \eta)dz_1 = O(1), \text{ for } \eta \in C_{F(a),\theta}$$

since $O(\eta_1) \int_{S_r} \frac{\ln(|z-\eta|)}{|z-\eta|} dz_1 = O(\frac{\eta_1}{\eta_2}) = O(1)$, for $\eta \in C_{F(a),\theta}$.

We consider now the second term: $\int_{S_r} [1 - |J^T \tilde{\nu}|](\nabla\Gamma \cdot \tau_2)(F^{-1}(z), F^{-1}(\eta))]G(z, \eta)dz_1$. Using the estimate $1 - |J^T \tilde{\nu}(z)| = O(z_1^2)$ and the expansions (61)-(62), its boundedness, for $\eta \in C_{F(a),\theta}$ small enough, is not difficult to see.

Proof of (70).

As for (69), we divide (70) as follows:

$$\int_{S_r} [\nabla_z(\nabla\Gamma \cdot \tau_2)(z, \eta) \cdot \tilde{\nu}(z) - \nabla_z(\nabla\Gamma \cdot \tau_2)(F^{-1}(z), F^{-1}(\eta)) \cdot \tilde{\nu}(z)]G(z, \xi)ds(z) + \int_{S_r} \nabla_z(\nabla\Gamma \cdot \tau_2)(F^{-1}(z), F^{-1}(\eta)) \cdot (\tilde{\nu}(z) - J^T \tilde{\nu}(z))G(z, \xi)ds(z).$$

Arguing as in the estimates used for proving (70), we obtain:

$$\begin{aligned} & \nabla_z(\nabla\Gamma \cdot \tau_2)(z, \eta) \cdot \tilde{\nu}(z) - \nabla_z(\nabla\Gamma \cdot \tau_2)(F^{-1}(z), F^{-1}(\eta)) \cdot \tilde{\nu}(z) \\ &= -\frac{\nu_1(a)}{\pi|z-\eta|^4} \left\{ \left(\frac{-4\eta_2^2}{|z-\eta|^2} + 1 \right) (z_1 - \eta_1)^2 f'_a(\eta_1) + \left(\frac{-2\eta_2^2}{|z-\eta|^2} + \frac{1}{2} \right) (z_1 - \eta_1)^3 f''_a(\eta_1) \right\} + \\ & \frac{-\nu_2(a)}{2\pi|z-\eta|^4} \left\{ \left(2 + \frac{4[(z_1 - \eta_1)^2 - \eta_2^2]}{|z-\eta|^2} \right) \eta_2 (z_1 - \eta_1) f'_a(\eta_1) + \left(1 + \frac{2[(z_1 - \eta_1)^2 - \eta_2^2]}{|z-\eta|^2} \right) \eta_2 (z_1 - \eta_1)^2 f''_a(\eta_1) \right\}. \end{aligned} \tag{76}$$

Estimating term by term, we obtain the boundedness of $\int_{S_r} [\nabla_z(\nabla\Gamma \cdot \tau_2)(z, \eta) \cdot \tilde{\nu}(z) - \nabla_z(\nabla\Gamma \cdot \tau_2)(F^{-1}(z), F^{-1}(\eta)) \cdot \tilde{\nu}(z)]G(z, \xi)ds(z)$ for $\eta \in C_{F(a),\theta}$ small enough.

To estimate the integral $\int_{S_r} \nabla_z(\nabla\Gamma \cdot \tau_2)(F^{-1}(z), F^{-1}(\eta)) \cdot (\tilde{\nu}(z) - J^T \tilde{\nu}(z))G(z, \xi)ds(z)$, we write:

$$\nabla_z(\nabla\Gamma \cdot \tau_2)(F^{-1}(z), F^{-1}(\eta)) \cdot \tilde{\nu}(z) = \nabla_z(\nabla\Gamma \cdot \tau_2)(z, \eta) \cdot \tilde{\nu}(z) + L(z, \eta)$$

where $L(z, \eta)$ is no thing but the expression (76) multiplied by -1. Since we already showed how the term $\int_{S_r} L(z, \eta)G(z, \eta)ds(z)$ is bounded for $\eta \in C_{F(a),\theta}$, then also $\int_{S_r} |\tilde{\nu}(z) - J^T \tilde{\nu}(z)|L(z, \eta)G(z, \eta)ds(z)$ is bounded for $\eta \in C_{F(a)}$ since $\tilde{\nu}(z) - J^T \tilde{\nu}(z)$ is bounded. Hence we need just to estimate $\int_{S_r} \nabla_z(\nabla\Gamma \cdot \tau_2)(z, \eta) \cdot (\tilde{\nu}(z) - J^T \tilde{\nu}(z))G(z, \xi)ds(z)$. We have $\tilde{\nu}(z) - J^T \tilde{\nu}(z) = (f'_a(z_1), 0)$, then

$$\nabla(\nabla\Gamma \cdot \tau_2)(z, \eta) \cdot (\tilde{\nu}(z) - J^T \tilde{\nu}(z)) = f'_a(z_1) \frac{\partial}{\partial z_1} \left[-\nu_1(a) \frac{\partial\Gamma}{\partial z_1} + \nu_2(a) \frac{\partial\Gamma}{\partial z_2} \right]$$

and hence

$$\nabla(\nabla\Gamma \cdot \tau_2)(z, \eta) \cdot (\tilde{\nu}(z) - J^T \tilde{\nu}(z)) = f'_a(z_1) \left[\frac{\nu_2(a)(z_1 - \eta_1)(z_2 - \eta_2)}{\pi|z-\eta|^4} - \frac{\nu_1(a)[(z_1 - \eta_1)^2 - (z_2 - \eta_2)^2]}{2\pi|z-\eta|^4} \right].$$

Knowing that $z_2 = 0$ on S_r and integrating term by term using the explicit forms of the integrands,

we prove that $\int_{S_r} \nabla_z (\nabla \Gamma \cdot \tau_2)(z, \eta) \cdot (\tilde{v}(z) - J^T \tilde{v}(z)) G(z, \xi) ds(z)$ is bounded for $\eta \in C_{F(a), \theta}$ small enough.

Step three. The estimate of $R(z, z)$ near the point a .

We go back to $R(x, z) := \tilde{E}_{\sigma(a), \Gamma}^{s, 0}(x, z) - w_{\sigma(a)}^+(x, z)$ and we write it as

$$R(x, z) = \tilde{R}(F(x), F(z)) + w_{\sigma(a)}^+(F(x), F(z)) - w_{\sigma(a)}^+(x, z).$$

From the previous computations, we have

$$\tilde{R}(F(z), F(z)) = O(1), \text{ for } z \in C_{a, \theta} \text{ near } a.$$

Due to the form of $w_{\sigma(a)}^+$, see Proposition 3.2, we prove that $w_{\sigma(a)}^+(F(z), F(z)) - w_{\sigma(a)}^+(x, z) = O(1)$, for $z \in C_{a, \theta}$ near a . Finally, we have

$$\tilde{E}_{\sigma(a), \Gamma}^{s, 0}(z, z) - w_{\sigma(a)}^+(z, z) = O(1), \text{ for } z \in C_{a, \theta} \text{ near } a.$$

The proof is complete. □

5. Numerical tests

In our model problem we take the crack as a half semi-circle with the representation

$$C = \{x : x = (x_1(s), x_2(s)) = 1.2 \times (\cos s, \sin s), s \in [0, \pi]\}. \tag{77}$$

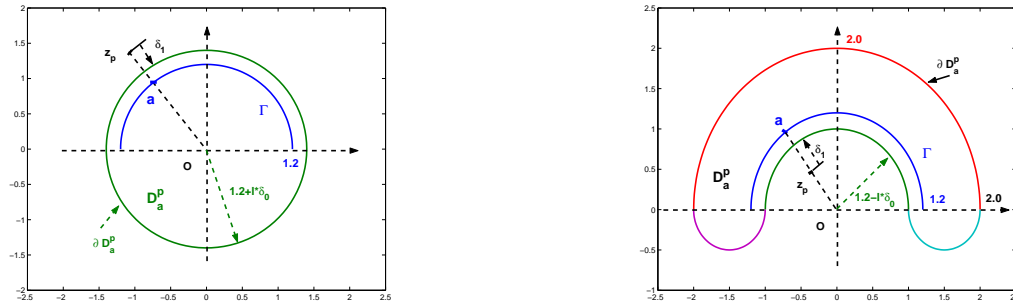


Figure 1. Construction of two D_a^p 's. z_p can approach C from its convex side using D_a^p in the left-hand side, while D_a^p in the right-hand side is used for z_p approaching C from its concave side. When $\delta_1 + l \times \delta_0 \rightarrow 0$ with l the approaching step at each direction, $z_p \rightarrow a \in C^\pm$ from both sides of C along radius direction, respectively.

We check the reconstruction formula for the scattering problem (3) which is the most difficult. The other two problems (1) and (2) can be checked in a similar way. In order to detect the crack C as well as its surface impedance σ_\pm , we need to construct some domain D_a^p such that $C \in D_a^p$ and z_p outside of D_a^p can approach C from its two sides. Notice, the choice of D_a^p depends on the *a-priori* information about the location and size of the unknown crack. For C given by (77), we construct

two kinds of D_a^p shown in Figure 1. Notice that the parameter $\delta_1 > 0$ represents the singularities of $\Phi(x, z_p)$, $\partial_{x_i} \Phi(x, z_p)$ for $x \in \partial D_a^p$ near z_p and $l \times \delta_0 > 0$ is the distance between \mathcal{C} and ∂D_a^p . The sum $\delta_1 + l \times \delta_0$ determines the approximation accuracy $|z_p - a|$ for $a \in \mathcal{C}$. On the other hand, it is easy to see that the domain D_a^p in the right-hand side can also be used for $z_p \rightarrow a \in \mathcal{C}$ from the convex part by translating D_a^p along x_2 direction.

We test our inversion method by showing the reconstructions for all the unknown ingredients in the model: the crack shape, crack type and surface impedance σ_{\pm} in two sides of the crack. We will consider different configurations to show the validity of the method and reveal the physical properties behind the numerical behavior. In fact, we will see that the crack property in the convex side can be distinguished efficiently, while the crack property in the concave side is relatively difficult to be reconstructed numerically. This phenomena comes from the multiple reflections for scattered waves in the concave parts of the crack and therefore more energy is absorbed.

Firstly, we use the blowing-up property of the indicator

$$Loc(z_p) := |\Re(I_1(z_p))| + |\Re(I_2(z_p))| \rightarrow +\infty \text{ as } z_p \rightarrow \mathcal{C} \quad (78)$$

to detect the location of crack due to (19). That is, when $Loc(z_p)$ is large enough, we consider z_p to be almost on \mathcal{C} .

Secondly, we use the following equivalent form of the reconstruction formulas (22) and (23)

$$\lim_{z_p \rightarrow a} \frac{\pi \sum_{j=1}^2 \nu_j(a) \Im(I_j(z_p))}{\kappa \ln(|(z_p - a) \cdot \nu(a)|)} = \begin{cases} -\sigma_+^r, & \text{if } z_p \rightarrow a \text{ from } \mathcal{C}^+ \\ \sigma_-^r, & \text{if } z_p \rightarrow a \text{ from } \mathcal{C}^-, \end{cases} \quad (79)$$

$$\begin{cases} \lim_{z_p \rightarrow a} \frac{\pi \sum_{j=1}^2 \nu_j(a) \Re(I_j(z_p)) - \frac{1}{4|(z_p - a) \cdot \nu(a)|}}{\kappa \ln(|(z_p - a) \cdot \nu(a)|)} = \sigma_+^i, & \text{if } z_p \rightarrow a \text{ from } \mathcal{C}^+ \\ \lim_{z_p \rightarrow a} \frac{\pi \sum_{j=1}^2 \nu_j(a) \Re(I_j(z_p)) + \frac{1}{4|(z_p - a) \cdot \nu(a)|}}{\kappa \ln(|(z_p - a) \cdot \nu(a)|)} = -\sigma_-^i, & \text{if } z_p \rightarrow a \text{ from } \mathcal{C}^- \end{cases} \quad (80)$$

for the surface impedance reconstruction as well as for distinguishing \mathcal{C}^+ from \mathcal{C}^- . This last property follows from (79) since σ^r is assumed to be positive. Hence if the left-hand side of (79) is positive then we are on the side \mathcal{C}^- and if not we are on the side \mathcal{C}^+ .

Finally, the crack type is shown by considering the blowing-up property of the function

$$Type(z_p) := \frac{|\Im(I_1(z_p))| + |\Im(I_2(z_p))|}{|\ln |(z_l - a) \cdot \nu(a)||^{1/2}} \text{ as } z_p \rightarrow \mathcal{C} \quad (81)$$

using the formula (21). That is, $Type(z_p)$ should increase up to some value (theoretically ∞) for the impedance crack.

In all the formulas (78)-(81), z_p are taken along the direction t_j to approach the point $a = R_0(\cos t_j, \sin t_j) \in \mathcal{C}$ for all t_j 's. In this way, the property of the crack is detected.

In our model problems we take the wave number $\kappa = 1.2$. The far-field pattern data for our inversion are synthesized by solving the direct problem using the combined angular potential and single-layer potential developed in [11].

Example 1 We take the surface impedance as the complex functions of the forms

$$\kappa\sigma_-(x) \equiv 1 + 1.5i, \quad \kappa\sigma_+(x) \equiv 2 + 1.2i \quad (82)$$

and use incident plan waves along 64 directions distributed uniformly in $[0, 2\pi]$.

Let $z_p = z(j, l)$ approach to \mathcal{C} from its convex side. By convex and concave side of crake, we mean the upper side and lower side of \mathcal{C} given by (77), respectively. The crack \mathcal{C} is detected

from 33 directions $t_j = \pi/32 \times j$ with $j = 0, 1, \dots, 32$. The radius for reconstruction at each direction t_j is determined by the following way. For given blowing-up criterion CB , let $z(j, l) = (\delta_1 + l \times \delta_0)(\cos t_j, \sin t_j)$ for $l = 16, 15, \dots, 1$. Here we take $\delta_1 = 0.01, \delta_0 = 0.02$. For any fixed $j = 0, 1, \dots, 32$, compute the indicator value $Loc(z(j, l))$ defined by (78). If this value is larger than CB the first time, we record this step $l(j)$ and the value $C_j := Loc(z(j, l(j)))$. Then we go to the next direction. Using this way, we get the data $\{l(j), C_j\}_{j=0}^{32}$. Compute the average value $C := \sum_{j=0}^{32} C_j/33$. Finally, we compare the value C_j and C and use this perturbation to correct the radius $R_0 + l(j) \times \delta_0$ by linear interpolation as $R_0 + l(j) \times \delta_0 - (C_j - C)/C \times \delta_0$. This is the final radius at direction t_j .

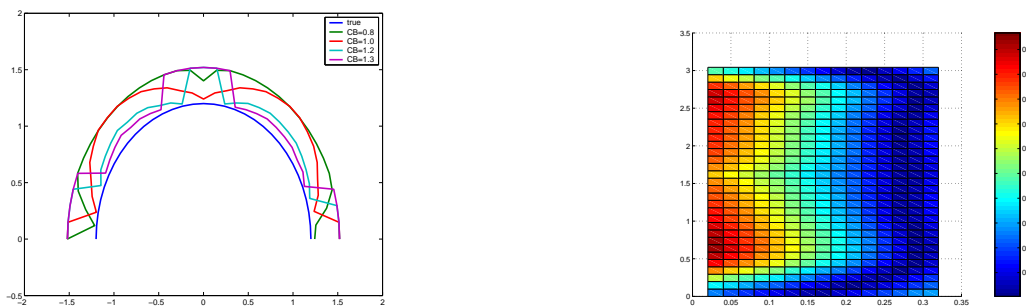


Figure 2. Construction of \mathcal{C} from the convex side of \mathcal{C} (left). It can be seen that the tips are not easy to identify with satisfactory accuracy. The crack type detection is shown in the right-hand side. The blowing-up property are shown obviously, except at the tips of the crack. It can be shown that the increasing property is quite weak when $z_p \rightarrow \mathcal{C}$ along direction $\theta \approx 1.57 \approx \pi/2$. This is reasonable, since $|\Im I_1(z_p)|$ in (81) is almost a constant as $z_p \rightarrow a$ along the direction $t = \pi/2$ and then the numerator in (81) is relatively small.

Take the blow-up parameter $CB = 0.8, 1.0, 1.2, 1.3$. The reconstruction results for crack location are given in the left-hand side of Figure 2 using the above procedure. Using the technique in [15], we can improve the reconstruction results by combining the reconstructions for different blowing-up criteria together. That is, when the concave closure for the reconstructions with different blowing-up values are taken, the crack will be detected from the convex side with a high accuracy. The only *a-priori* information about the crack is that we know that z_p is in the upper-side of the crack. Notice, in our setting here $\sigma_+^i > 0$. To use our reconstruction formula (21) more efficiently, we expect that the reconstruction will be much improved for the case $\sigma_+^i < 0$. However, we need to clarify the physical meaning of this condition. To our knowledge, all the reconstruction problems for surface impedance up to now always consider the case $\sigma_+^i \equiv 0$.

The crack type detection is checked using (81) with the numerical performance given in the right-hand side of Figure 2. The blowing-up property are shown obviously, except at the tips of the crack. Notice, here we use the same singularity to identify the arc shape and the boundary type. It can be shown that the increasing property is quite weak when $z_p \rightarrow \mathcal{C}$ along direction $\theta \approx 1.57 \approx \pi/2$. This is reasonable since $\nu_1(a) = 0$ for $a = 1.2(\cos \frac{\pi}{2}, \sin \frac{\pi}{2})$. Therefore $|\Im I_1(z_p)|$ in (81) is almost a constant as $z_p \rightarrow a$ along the direction $t = \pi/2$ and then the numerator in (81) is relatively small, compared with those along other directions.

Now let us recover the boundary impedances σ_{\pm} . We need to apply different singularity to detect its real part and imaginary part, respectively.

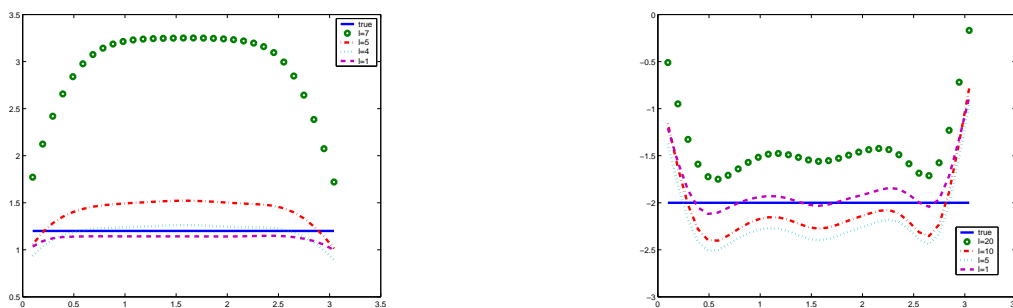


Figure 3. Construction of σ_+ from the convex side of \mathcal{C} : imaginary part $\kappa\sigma_+^i$ (left) and real part $-\kappa\sigma_+^r$ (right). The reconstructions are satisfactory except at the tips of the crack, the approximation effect is nice for small l which means the detecting point approaches to the crack.

We take $\delta_0 = 0.1, \delta_1 = 0.025$ for recovering the imaginary part of σ_+ . The reconstruction results for $l = 7, 5, 4, 1$ are shown in the left-hand side of Figure 3 noticing $\delta_0 = 0.1$ and the radius of crack is 1.2. For recovering the real part of σ_+ , we need a strong singularity. Here we take $\delta_0 = 0.01, \delta_1 = 0.003$. The reconstruction for $l = 20, 10, 5, 1$ are given in the right-hand side of Figure 3. Notice that the numerical performance is not monotone with respect to l for both real part and imaginary part. Although there are some oscillations for real part of σ_+ , the reconstruction is satisfactory.

Next we will check the reconstruction of σ_- . Since σ_- is defined in the concave part of \mathcal{C} , we use D_a^p shown in the right-hand side of Figure 1. For recovering its imaginary part, we take $\delta_0 = 0.03, \delta_1 = 0.01$. The results for $l = 8, 4, 2, 1$ are shown in the left-hand side of Figure 4.

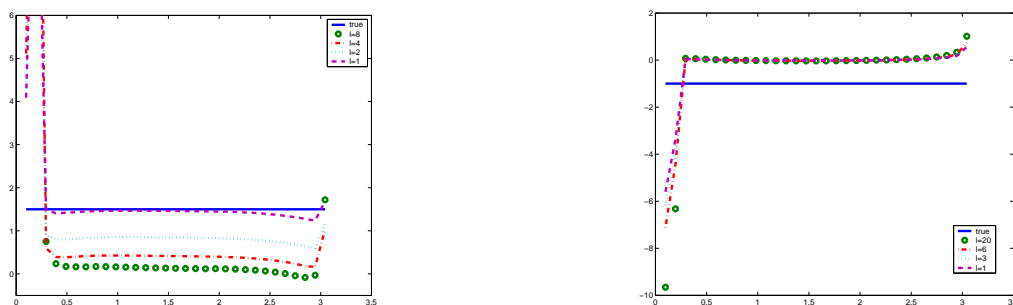


Figure 4. Construction of σ_- from the concave side of \mathcal{C} : imaginary part $\kappa\sigma_-^i$ (left) and real part $-\kappa\sigma_-^r$ (right). The imaginary part is reconstructed well. For real part, we can only get the distribution behavior, rather than the exact value.

Huge jumps appear at the tips. To show these huge jumps, we list the values near the two tips as follows.

Tab.4.1 Numerical behavior of reconstructing σ_- near the tips.

	$j = 1$	$j = 2$	$j = 3$	$j = 30$	$j = 31$
$l = 8$	8.769352	35.33823	0.7525697	-3.0021202E-02	1.719347
$l = 4$	5.030425	19.36075	0.5959290	0.1632772	1.036119
$l = 2$	4.122960	14.12117	0.9113938	0.6005412	1.183656
$l = 1$	4.087763	12.01402	1.487852	1.236337	1.686392

For recovering the real part of σ_- , we take $\delta_0 = 0.002, \delta_1 = 0.001$, a stronger singularity. The results for $l = 20, 6, 3, 1$ are shown in Figure 4 (right). It can be seen that distribution behavior of σ_-^r is well detected, but the exact value can not be reconstructed well. This phenomena for recovering σ_-^r can also be shown from the other sets of (δ_0, δ_1) with

$$\delta_0 = \delta_1 = 10^{-i}, \quad i = 1, 2, 3, 4$$

for $l = 1$, that is, the approximate point is of the distance $\delta_0 + \delta_1$ from the boundary. The results as well as its refinement are given in Figure 5.

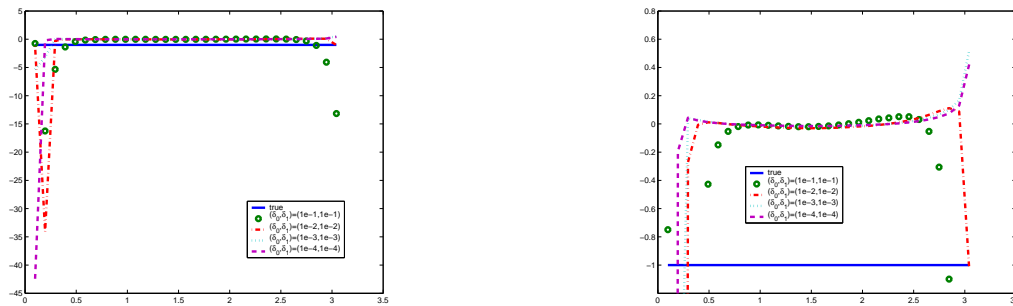


Figure 5. Reconstruction for σ_-^r for different sets of (δ_0, δ_1) (left), the right-hand side is its refinement. It can be seen that σ_-^r can not be recovered numerically. However, the distribution behavior of σ_-^r in the interior part of crack is well detected.

The physical background behind this numerical uncertainty for recovering σ_-^r is the multiple reflections of scattered wave in the cavity of the crack \mathcal{C} in its concave side. Near these concave points, the incident wave will be multi-reflected. For our impedance crack with the energy absorbing coefficient σ_-^r in the concave side, the energy of scattered wave is decreased by each reflection. Therefore the information about the concave side of the crack contained in the far-field pattern is also relatively decreased. We observe also that the multiple reflection of the concave side of the whole crack for a given σ_-^r has the same effects as the other non-concave part of the crack with a higher σ_-^r distribution. Such an energy absorbing phenomena is also studied by engineering, see [7] and the references therein.

Due to these reasons, it is understandable that we can not expect too much about the shape reconstruction from the concave side of the crack. Two reconstruction results using formula (78) using $z_p \rightarrow a \in \mathcal{C}$ from the concave side with $\delta_0 = 0.02, \delta_1 = 0.001$ and $\delta_0 = 0.02, \delta_1 = 0.01$ are shown in Figure 6 and Figure 7, respectively. In these two figures, we also take $l = 16, \dots, 1$.

It can be seen that the parts near the two tips can not be identified in the same way as the interior points of the crack. Actually, there is more scattering on these tips than on the interior points on the crack. Notice that the formulas given in section 2 are valid just on the points away from the tips. Also the best approximation accuracy can not be improved. What we can expect is that more part

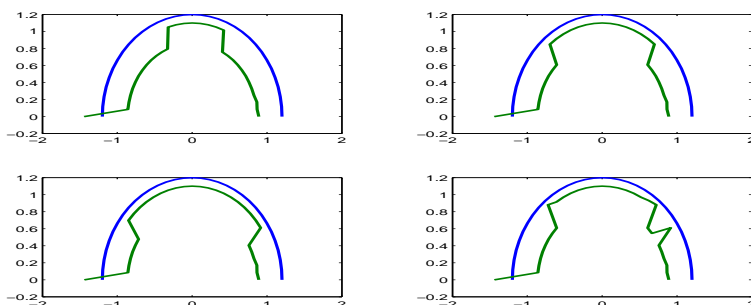


Figure 6. Reconstruction of the crack from the concave side using the singularity $\delta_0 = 0.02$, $\delta_1 = 0.001$, where the blowing-up criteria are taken as $CB = 0.2, 0.4, 0.9, 1.0$, from left to right in the first row and then in the second row.

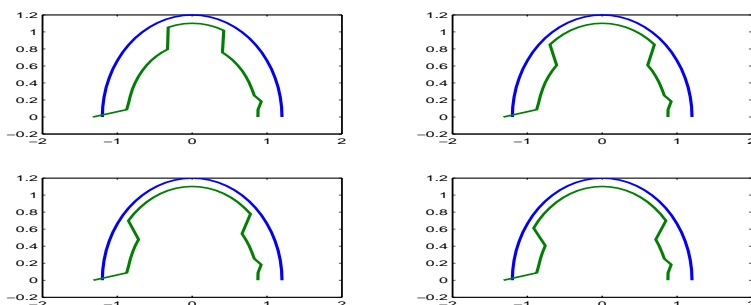


Figure 7. Reconstruction of the crack from the concave side using $\delta_0 = 0.02$, $\delta_1 = 0.01$, where the blowing-up criteria are taken as $CB = 0.2, 0.4, 0.6, 0.8$, from left to right in the first row and then in the second row.

of the crack will be visible using a larger CB but with a finite accuracy. In this configuration, we can not get the blowing-up property of the indicator value numerically since for $\delta_0 = 0.02$ and large l , the distance between z_p and the crack is still large, while the blowing-up property is established theoretically for $l \times \delta_0 + \delta_1 \rightarrow 0$.

Our next example is to consider the reconstruction problem where the surface impedance distribution is not constant in the surface, which shows the practical applicability of our reconstruction method.

Example 2. The configuration is taken as follows:

$$\kappa\sigma_+(x) = (\cos^2(x_1 + x_2) + 1.2) + i(\sin \frac{x_1 + x_2}{10} + 1.5), \quad \kappa\sigma_-(x) = (x_1 + 2) + ix_2 \quad (83)$$

for $x = (x_1, x_2) \in \mathcal{C}$. The real parts of σ_{\pm} are positive. The distribution of $\kappa\sigma_+$ are shown in Figure 8. Since we can not expect satisfactory results for the information about \mathcal{C}_- as explained in Example 1, here we focus on the reconstruction of σ_+ as well as the shape detection from the convex side of crack. We will reveal the effect of the variable surface impedance on the crack shape detection.

We use singularities $\delta_0 = 0.02, 0.01$ to detect the crack shape. The reconstruction result is shown in Figure 9 (left). It can be seen that the reconstruction in domain A is relatively poor. This domain

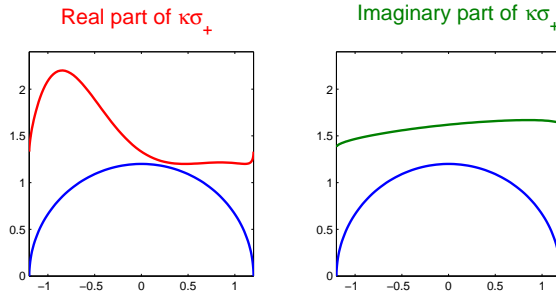


Figure 8. The non-constant distribution of $\kappa\sigma_+$ with respect to variable x_1 : real part(left) and imaginary part (right). The half circle represents the crack.

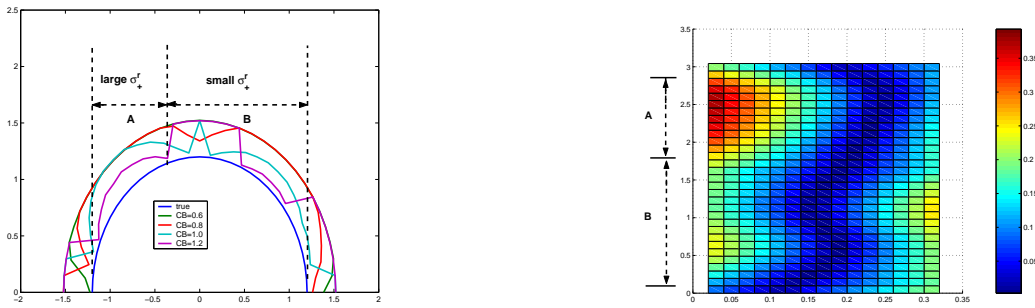


Figure 9. Reconstruction of \mathcal{C} using $(\delta_0, \delta_1) = (0.02, 0.01)$ with $CB = 0.6, 0.8, 1.0, 1.2$ (left). The crack shape in domain A is not easy to detect due to the large σ_+^r in this part, see the recovery for $CB = 1.0, 1.2$. It can be seen that absorbing property of σ_+^r helps us to detect the boundary type obviously. That is, in domain A with large value of σ_+^r , the blowing-up property is obvious. This phenomena is consistent with the detecting formula (20).

is the part where we have a large value of $\Re \sigma_+$, compare with Figure 8. The large value of σ_+^r in this domain means a large energy absorbing of the scattered wave. So we can not detect this part using the same singularity as that for the other part. Since σ_+^r is relatively small in the domain B , the shape detection is well in this part.

As it is done in Example 1, we use the same singularity to detect the boundary type. The numerical behavior of (81) in this case is shown in the right-hand side of Figure 9. The vertical variable is the detection direction $t_j = \pi/32 \times j$ for $j = 0, 1, \dots, 32$.

Finally, we reconstruct σ_+ . To recover the imaginary part of σ_+ , we use the singularity $\delta_0 = 0.02, \delta_1 = 0.03$. The results for $l = 20, 4, 2, 1$ are given in the left-hand side of Figure 10. Also we use the singularity $\delta_0 = 0.003, \delta_1 = 0.002$ to detect the real part of σ_+ . The results for $l = 20, 10, 5, 1$ are given in the right-hand side of Figure 10.

Example 3: This example is for showing the importance of introducing the artificial coefficient $\Im\sigma_{\pm} \neq 0$ in the surface impedance. We keep the other parameters in Example 1 unchanged and we replace the impedance by

$$\sigma_-(x) \equiv 1 + 2i, \sigma_+(x) \equiv 2 + 5i.$$

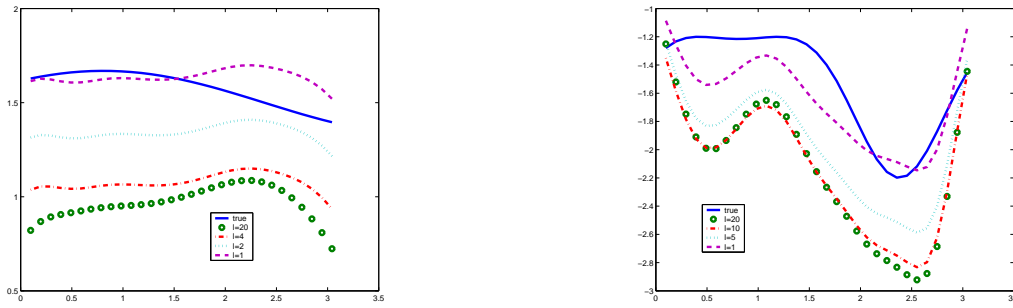


Figure 10. Construction of σ_+ from the convex side of \mathcal{C} : Imaginary part $\kappa\sigma_+^i$ (left) and real part $-\kappa\sigma_+^r$ (right). The numerical oscillation in reconstructing the real part of σ_+ is obvious.

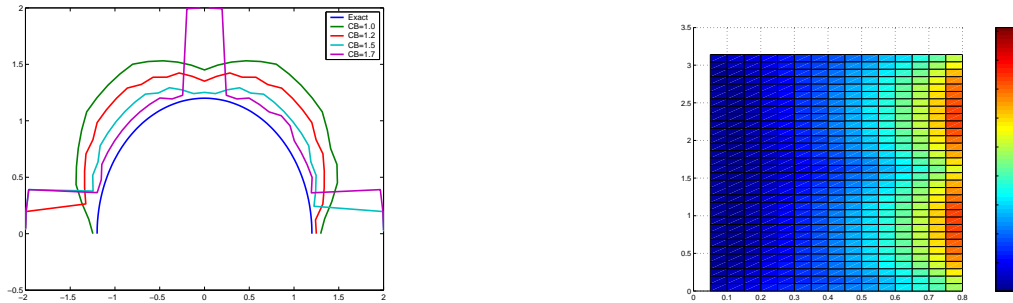


Figure 11. Boundary shape reconstruction and boundary type using the same singularity. The boundary shape is reconstructed well (left). Since σ_{\pm} are large, the crack behaves like a Dirichlet crack., i.e. $Type(z_p) \approx 0$. This phenomena is shown in the right-hand side of Figure 11.

The arc \mathcal{C} is reconstructed in Figure 11 (left). The blow-up values are $CB = 1.0, 1.2, 1.5, 1.7$, where we take $z(l) = l \times 0.05$ for $l = 16, 15, \dots, 1$ to approach $a \in \mathcal{C}$ with $\delta_1 = 0.1$. The reconstruction for crack shape is much better than Example 1 due to the large imaginary part of σ_{\pm} . Notice that this picture shows that the points near $(0, 1.2)$ can not be reconstructed well. The reason is that the normal direction is $\nu = (0, 1)$, which means $\nu_1 = 0$. The figure in the right-hand side of Figure 11 shows the boundary detection.

Conclusions. In this paper, we consider an inverse scattering problem by an open crack \mathcal{C} . Compared with the inverse scattering problem by an impenetrable obstacle with smooth closed boundary, the crack detection problems are much more complicated, due to the joint effects of the tips of crack, the concave side of crack and the inhomogeneous surface impedance distributions. We propose theoretical formulas to detect the properties of the crack such as its shape, the boundary type and the surface impedance. The numerical realizations are presented, which show the validity of this method and also some difficulties arising in the detection of concave side of crack. Such difficulties can be explained physically from the multiple reflection of waves in the cavity.

ACKNOWLEDGEMENTS

The first author is supported by NSFC (No.10771033) and also thanks RICAM (of the Austrian academy of sciences) for the hospitality during his visit in 2007. The second author is supported by the Austrian academy of sciences and the FWF through the SFB project F1308.

REFERENCES

1. K. BRYAN, M. S. VOGELIUS, *A review of selected works on crack identification*, Geometric methods in inverse problems and PDE control, IMA Math. Appl., Vol.137, 25-46, 2004.
2. F. CAKONI, D. COLTON, *Qualitative Methods in Inverse Scattering Theory*, Interaction of Mechanics and Mathematics, Springer, 2006.
3. D. COLTON, R. KRESS, *Inverse Acoustic and Electromagnetic Scattering Theory*, 2nd edition, Berlin-Springer, 1998.
4. M. GRUTER, K. O. WIDMAN, *The Green function for uniformly elliptic equations*, Manuscripta Math, Vol.37, 303-342, 1982.
5. M. IKEHATA, *Inverse crack problem and probe method*, Cubo 8, No.1, 29-40, 2006.
6. M. IKEHATA, G. NAKAMURA, *Reconstruction formula for identifying cracks*, Essays and papers dedicated to the memory of Clifford Ambrose Truesdell III, Vol.II. J. Elasticity, Vol.71, No. 1-3, 59-72, 2003.
7. K. GOTO, T. ISHIHARA, *High-frequency (Whispering-Gallery Mode)-to-beam conversion on a perfectly conducting concave-convex boundary*, IEEE Transactions on Antennas and Propagation, Vol.50, No.8, 1109-1119, 2002.
8. P.A. KRUTITSKII, *Dirichlet's problem for the Helmholtz equation outside cuts in a plane*, Computational Math and Mathematical Physics, Vol.34, No.8/9, 1073-1090, 1994.
9. P.A. KRUTITSKII, V.V. KOLYBASOVA, *The Helmholtz equation outside cuts on the plane with the Dirichlet condition and a third kind boundary condition on opposite sides of the cuts*, Differential Equations, Vol.42, No.9, 1247-1261, 2006.
10. P.A. KRUTITSKII, *The Helmholtz equation in the exterior of slits in a plane with different impedance boundary conditions on opposite sides of the slits*, Quart. Appl. Maths, Vol.66, No.4, 2008.
11. P.A. KRUTITSKII, J.J. LIU AND M. SINI, *Numerical solution of the scattering problem for acoustic waves by a two-sided crack in 2-dimensional space*. Preprint.
12. P.A. KRUTITSKII, J.J. LIU AND M. SINI, *Reconstruction of complex cracks by exterior measurements*, 6th International Conference on Inverse Problems in Engineering: Theory and Practice, Paris, J. Physics: Conference Series, Vol.135, doi:10.1088/1742-6596/135/1/012056, 2008.
13. R. KRESS, K.M. LEE, *Integral equation methods for scattering from an impedance crack*, J. Comput. Appl. Math. Vol.161, No.1, 161-177, 2003.
14. W. LITTMAN, G. STANPACCHIA AND H. F. WEINBERGER, *Regular points for elliptic equations with discontinuous coefficients*, Ann. Scuola Norm. Sup. Pisa (III), Vol.17, 43-77, 1963.
15. J.J. LIU, G. NAKAMURA AND M. SINI, *Reconstruction of the shape and surface impedance from acoustic scattering data for an arbitrary cylinder*, SIAM J. Appl. Math. Vol.67, No.4, 1124-1146, 2007.
16. W. MCLEAN, *Strongly Elliptic Systems and Boundary Integral Equations*, Cambridge University Press, 2000.
17. G. NAKAMURA, M. SINI, *Obstacle and boundary determination from scattering data*, SIAM J. Math. Anal. Vol.39, No.3, 819-837, 2007.
18. R. POTTHAST, *Point Sources and Multipoles in Inverse Scattering Theory*, Research Notes in Mathematics, Vol.427, Chapman-Hall/CRC, Boca Raton, FL, 2001.
19. V. A. SOLONNIKOV, *On Green's matrices for elliptic boundary value problems(I)*, Proc. Steklov. Inst. Math., Vol.110, 1970.
20. V. A. SOLONNIKOV, *The Green's matrices for elliptic boundary value problems(II)*, Boundary Value Problems of Mathematical Physics, 7, Trudy. Math. Inst. Steklov., Vol.116, 181-216, 1971.